



# Cyclophilin A is a ligand for RAGE in thrombo-inflammation

Peter Seizer<sup>1,2†</sup>, Saskia N.I. von Ungern-Sternberg<sup>1†</sup>, Verena Haug<sup>1</sup>, Valerie Dicenta<sup>1</sup>, Annabelle Rosa<sup>3</sup>, Elke Butt<sup>3</sup>, Moritz Nöthel<sup>4</sup>, Anne-Katrin Rohlfing <sup>1</sup>, Manuel Sigle<sup>1</sup>, Peter P. Nawroth<sup>5,6,7</sup>, Claudia Nussbaum<sup>8</sup>, Markus Sperandio<sup>9,10</sup>, Charly Kusch<sup>3</sup>, Mara Meub<sup>11</sup>, Markus Sauer<sup>11</sup>, Patrick Münzer<sup>1,12</sup>, Kristin Bieber<sup>13</sup>, Anna Stanger<sup>13</sup>, Andreas F. Mack<sup>14</sup>, René Huber<sup>15</sup>, Korbinian Brand<sup>15</sup>, Moritz Lehnert<sup>16</sup>, Robert Feil<sup>16</sup>, Antti Poso<sup>17,18,19,20,21,22</sup>, Konstantin Krutzke<sup>23</sup>, Tilman E. Schäffer<sup>23</sup>, Bernhard Nieswandt<sup>3,24</sup>, Oliver Borst<sup>1,12</sup>, Andreas E. May<sup>25</sup>, Alma Zerneck<sup>3</sup>, Meinrad Gawaz<sup>1</sup>, and David Heinzmann <sup>1\*</sup>

<sup>1</sup>Department of Cardiology and Angiology, Universitätsklinikum Tübingen, Eberhard Karls University Tübingen, Otfried-Müller-Str. 10, 72076 Tübingen, Germany; <sup>2</sup>Department of Cardiology and Angiology, Ostalbklinikum Aalen, Aalen, Germany; <sup>3</sup>Institute of Experimental Biomedicine, University Hospital Würzburg, Würzburg, Germany; <sup>4</sup>Department of Internal Medicine II, Cardiology, Pneumology, Angiology, University Hospital Bonn, Bonn, Germany; <sup>5</sup>Department of Internal Medicine 1 and Clinical Chemistry, University Hospital of Heidelberg, Heidelberg, Germany; <sup>6</sup>German Center for Diabetes Research (DZD), Munich-Neuherberg, Germany; <sup>7</sup>Joint Heidelberg-ICD Translational Diabetes Program, Helmholtz-Zentrum, Munich, Germany; <sup>8</sup>Division of Neonatology, Department of Pediatrics, Dr. von Hauner Children's Hospital, LMU University Hospital, LMU Munich, Munich, Germany; <sup>9</sup>Institute of Cardiovascular Physiology and Pathophysiology, Ludwig-Maximilians University Munich, Munich, Germany; <sup>10</sup>German Centre for Cardiovascular Research (Deutsches Zentrum für Herz-Kreislauf-Forschung, DZHK), Munich Heart Alliance Partner Site, Munich, Germany; <sup>11</sup>Department of Biotechnology and Biophysics, Julius-Maximilians University, Würzburg, Germany; <sup>12</sup>DFG Heisenberg Group Cardiovascular Thromboinflammation and Translational Thrombocardiology, University of Tübingen, Tübingen, Germany; <sup>13</sup>Department of Hematology, Oncology, Immunology und Pulmonology, Universitätsklinikum Tübingen, Eberhard Karls University Tübingen, Tübingen, Germany; <sup>14</sup>Institute of Clinical Anatomy and Cell Analytics, Eberhard Karls University Tübingen, Tübingen, Germany; <sup>15</sup>Institute of Clinical Chemistry, Hannover Medical School, Hannover, Germany; <sup>16</sup>Interfakultäres Institut für Biochemie, Eberhard Karls University Tübingen, Tübingen, Germany; <sup>17</sup>Department of Internal Medicine VIII, University Hospital of Tübingen, Tübingen, Germany; <sup>18</sup>School of Pharmacy, Faculty of Health Sciences, University of Eastern Finland, Kuopio, Finland; <sup>19</sup>Department of Pharmaceutical and Medicinal Chemistry, Institute of Pharmaceutical Sciences, Eberhard Karls University Tübingen, Tübingen, Germany; <sup>20</sup>Department of Pharmaceutical and Medicinal Chemistry, Institute of Pharmaceutical Sciences, Eberhard Karls University, Tübingen, Germany; <sup>21</sup>Tübingen Center for Academic Drug Discovery & Development (TüCAD2), Tübingen, Germany; <sup>22</sup>Excellence Cluster 'Controlling Microbes to Fight Infections' (CMFI), Tübingen, Germany; <sup>23</sup>Institute of Applied Physics, Eberhard Karls University Tübingen, Tübingen, Germany; <sup>24</sup>Rudolf Virchow Center, University of Würzburg, Würzburg, Germany; and <sup>25</sup>Department of Cardiology, Innere Medizin I, Klinikum Memmingen, Memmingen, Germany

Received 30 January 2023; revised 8 October 2023; accepted 20 October 2023; online publish-ahead-of-print 4 January 2024

Time of primary review: 27 days

## Aims

Cyclophilin A (CyPA) induces leucocyte recruitment and platelet activation upon release into the extracellular space. Extracellular CyPA therefore plays a critical role in immuno-inflammatory responses in tissue injury and thrombosis upon platelet activation. To date, CD147 (EMMPRIN) has been described as the primary receptor mediating extracellular effects of CyPA in platelets and leucocytes. The receptor for advanced glycation end products (RAGE) shares inflammatory and prothrombotic properties and has also been found to have similar ligands as CD147. In this study, we investigated the role of RAGE as a previously unknown interaction partner for CyPA.

## Methods and results

Confocal imaging, proximity ligation, co-immunoprecipitation, and atomic force microscopy were performed and demonstrated an interaction of CyPA with RAGE on the cell surface. Static and dynamic cell adhesion and chemotaxis assays towards extracellular CyPA using human leucocytes and leucocytes from RAGE-deficient *Ager*<sup>-/-</sup> mice were conducted. Inhibition of RAGE abrogated CyPA-induced effects on leucocyte adhesion and chemotaxis *in vitro*. Accordingly, *Ager*<sup>-/-</sup> mice showed reduced leucocyte recruitment and endothelial adhesion towards CyPA *in vivo*. In wild-type mice, we observed a downregulation of RAGE on leucocytes when endogenous extracellular CyPA was reduced. We furthermore evaluated the role of RAGE for platelet activation and thrombus formation upon CyPA stimulation. CyPA-induced activation of platelets was found to be dependent on RAGE, as inhibition of RAGE, as well as platelets from *Ager*<sup>-/-</sup> mice showed a diminished activation and thrombus formation upon CyPA stimulation. CyPA-induced signalling through RAGE was found to involve central signalling pathways including the adaptor protein MyD88, intracellular Ca<sup>2+</sup> signalling, and NF-κB activation.

\*Corresponding author. Tel: +49 7071 29 83688; fax: +49 7071 29 5749, E-mail: [david.heinzmann@med.uni-tuebingen.de](mailto:david.heinzmann@med.uni-tuebingen.de)

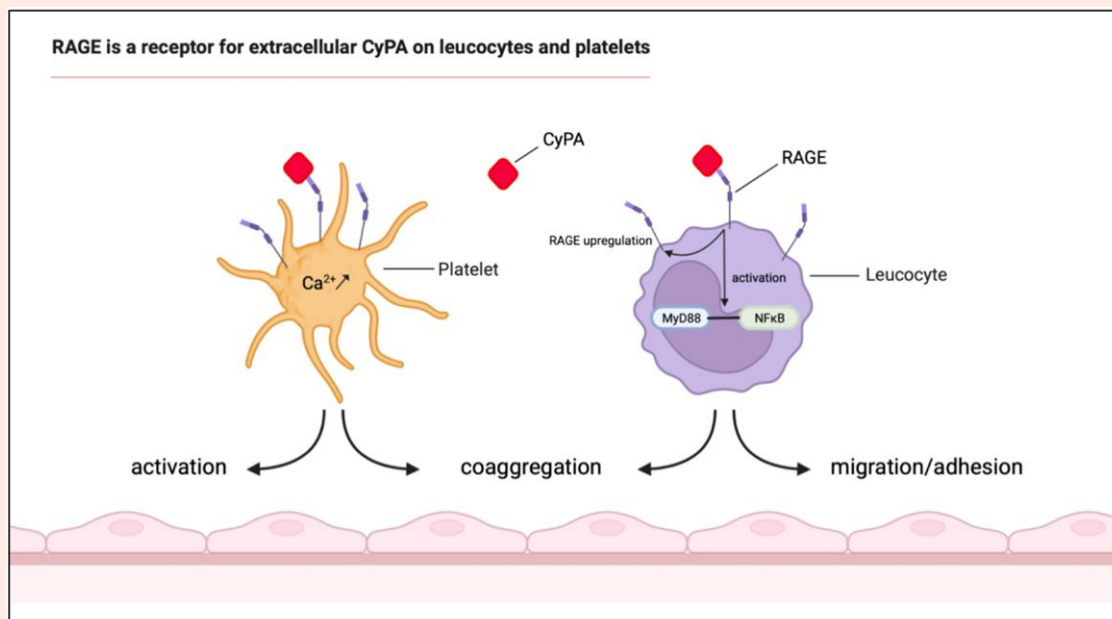
† The first two authors contributed equally to the study.

© The Author(s) 2024. Published by Oxford University Press on behalf of the European Society of Cardiology. All rights reserved. For permissions, please e-mail: [journals.permissions@oup.com](mailto:journals.permissions@oup.com)

## Conclusion

We propose RAGE as a hitherto unknown receptor for CyPA mediating leucocyte as well as platelet activation. The CyPA–RAGE interaction thus represents a novel mechanism in thrombo-inflammation.

## Graphical Abstract



RAGE is a novel receptor for extracellular CyPA on leucocytes and platelets. RAGE was found to interact with CyPA and to play an important role in CyPA-induced leucocyte and platelet functions. Platelet activation, coaggregate formation, and intracellular  $Ca^{2+}$  release by CyPA were abrogated when RAGE was absent or blocked. Similarly, CyPA-induced leucocyte migration and adhesion were found to be dependent on RAGE *in vivo* and *in vitro*. CyPA abundance was furthermore identified to regulate RAGE expression *in vivo*.

## Keywords

Cyclophilin A • RAGE • Platelets • Leucocytes • Thrombosis • Inflammation

## 1. Introduction

Cyclophilin A (CyPA) is a well-characterized primarily intracellular 18 kDa peptidyl-prolyl isomerase, which has been identified to play an important role in a broad range of inflammatory diseases, neurodegeneration, cancer, viral infection, cardiovascular disorders, and asthma.<sup>1–10</sup> While being an important intracellular target for the immunosuppressive drug cyclosporine, CyPA can be released into the extracellular space in response to various proinflammatory conditions including necrosis, reactive oxygen species (ROS), lipopolysaccharides (LPS) stimulation, and irradiation.<sup>11–13</sup> Extracellular CyPA is a strong chemoattractant inducing leucocyte chemotaxis, adhesion, and secretion of matrix metalloproteinases. Furthermore, extracellular CyPA has been identified as an inducer of platelet activation and thrombosis and beyond their role in haemostasis and pathological arterial thrombus formation, emerging evidence supports the pivotal role of platelets in inflammation, cellular repair, and fibrosis.<sup>14–19</sup>

To date, CD147 (EMMPRIN), being expressed on many different cell types including leucocytes and platelets, has been the primary interaction partner identified to mediate effects of extracellular CyPA, inducing downstream modification of key pathways, especially NF- $\kappa$ B activation.<sup>3,4,20</sup>

Recently, S100A9 has been reported to not only interact with receptor for advanced glycation end products (RAGE) but also with CD147, promoting tumour metastasis and monocyte/macrophage migration.<sup>21,22</sup> We were therefore intrigued to investigate whether RAGE, similar to

CD147, could be a receptor for extracellular CyPA in the context of thrombo-inflammation.

Since its discovery in 1992, many different ligands apart from advanced glycation end products (AGEs) have been identified, making RAGE a pattern recognition receptor.<sup>23</sup> Among these are members of the S100 protein family, HMGB1, amyloid- $\beta$ , and others.<sup>24–27</sup> RAGE activation facilitates proinflammatory effects, including NF- $\kappa$ B activation, formation of ROS, leucocyte recruitment, and apoptosis.<sup>28,29</sup> RAGE is furthermore expressed on platelets and has been found to augment their activation in various pathophysiological mechanisms.<sup>30–33</sup> Both for RAGE and CD147, signal transduction has been found to be very complex. CD147 requires for its proper function a metabolic activation complex consisting of amino acid transporters 4F2hc, LAT1, and ASCT2 (SLC1A5),  $Na^+/K^+$ -ATPase, and the cell adhesion mediators EpCAM and integrin  $\beta$ 1, termed a 'metabolon'.<sup>34</sup> For RAGE, transactivation without binding of a ligand has been shown through other receptors, and it has been identified to play a complex role in the directional crosstalk enabling downstream signal transduction.<sup>35</sup> RAGE is therefore an intricate player in the pathophysiology of inflammatory processes, including diabetes mellitus, myocardial ischaemia–reperfusion injury, allergy, rheumatological diseases, and others.<sup>27,36–38</sup> Especially in the context of cardiovascular disease, the interaction of RAGE and CyPA could therefore be of significant interest to better understand pathophysiological changes and potentially develop new therapeutic strategies.

In the current study, we provide evidence that RAGE is critically involved in CyPA-mediated proinflammatory and prothrombotic mechanisms *in vitro* and *in vivo*, offering new insight into crosslinks of thrombo-inflammatory processes.

## 2. Methods

### 2.1 Ethics statement and data availability

All animal experiments were performed according to the animal protection law of Germany and to the guidelines from Directive 2010/63/EU of the European Parliament on the protection of animals used for scientific purposes and were approved by local ethics committees. *Ager*<sup>-/-</sup> (B6.129P2-Ager<sup>tm1.1Arnd</sup>, 2–12 months old), *MyD88*<sup>-/-</sup> [B6.129P2(SJL)-*MyD88*<sup>tm1.1D<sup>efr</sup></sup>], 3 months old], and C57BL/6 mice were used in the experiments. All efforts were made to minimize suffering; euthanasia was performed by isoflurane (5% v/v) or ketamine (100 mg/kg body weight) and xylazine (20 mg/kg body weight) anaesthesia with subsequent exsanguination or cervical dislocation. Investigators were blinded to the treatment of animals. All experiments on human material were approved by the local ethics committee (270/2011BO1, 238/2018BO2) and were conducted in accordance to the principles outlined in the Declaration of Helsinki; informed written consent was given prior to the inclusion of subjects in the study.

### 2.2 Isolation of human monocytes

Human monocytes were isolated as previously described.<sup>4</sup> Briefly, peripheral blood was drawn from healthy donors in CPDA monovettes (Sarstedt) and centrifuged in a Ficoll gradient (GE Healthcare) to separate the leucocytes. Leucocytes were allowed to adhere overnight, and adherent monocytes were harvested. The cells were cultured in RPMI 1640 medium (Gibco) supplemented with 10% foetal calf serum (Gibco) and 100 U/mL penicillin and 100 µg/mL streptomycin (both Sigma-Aldrich) in a 5% CO<sub>2</sub> humidified atmosphere at 37°C.

### 2.3 Isolation of murine leucocytes

Murine leucocytes were isolated from bone marrow or whole blood of 2–12 months old mice. The bone marrow was washed with RPMI 1640 medium, supplemented with 10% foetal calf serum, 1% HEPES, 100 U/mL penicillin, 100 µg/mL streptomycin, and 0.01% granulocyte-macrophage colony-stimulating factor (GM-CSF). Erythrocytes were lysed in ammonium chloride. Cells were resuspended in supplemented medium and cultured in six-well plates in a 5% CO<sub>2</sub> humidified atmosphere at 37°C.

### 2.4 Confocal microscopy

For colocalization experiments, human monocytes were isolated and allowed to adhere on poly-L-lysine-coated chamber slides. Cells were stimulated with 200 nM recombinant CyPA (R&D Systems) and fixed with 4% formalin. After blocking monocytes with 10% donkey serum in phosphate buffered saline (PBS), the cells were incubated with antibodies against RAGE (Abcam, R&D Systems), CD147 (Abcam), or IgG controls overnight at 4°C. Cells were incubated with Alexa Fluor 488 or Alexa Fluor 568-labelled secondary antibodies (Life Technologies), and the nucleus was stained using DAPI. The cells were mounted using Fluorescent Mounting Medium (Thermo Fisher). Images were taken on a ZEISS LSM 900 with Airyscan 2. Micrographs shown represent single plane images. Analysis of colocalization of RAGE and CD147 was performed using Zeiss colocalization software.

### 2.5 Proximity ligation assay

Proximity ligation assays (Duolink PLA, Merck) were performed according to the manufacturer's instructions with human monocytes ( $n \geq 2$  biological replicates) or murine leucocytes from *Ager*<sup>-/-</sup> or wild-type mice ( $n = 4$  biological replicates) as indicated. Primary antibodies against CyPA, RAGE, or CD147 control were bound by oligonucleotide-labelled secondary antibodies. Hybridizing connector oligos can only join the two antibody-bound

oligos if they are in close proximity to each other. In the next step, a ligase formed a closed circular DNA template that was the template for a rolling circle amplification. Labelled oligos were hybridized to the complementary sequences within the amplicon, which allowed a strong signal amplification. Cells were stimulated with recombinant 200 nM CyPA (R&D Systems) in the presence or absence of the RAGE inhibitors FPS-ZM1 (300 nM, Merck), RAGE-antagonistic peptide (RAP; 300 nM, Merck), solvent, or IgG controls as indicated and afterwards fixed with 2% formalin. After blocking with 10% donkey serum in PBS, the cells were incubated with antibodies against RAGE (Abcam, R&D Systems), CD147 (Abcam), and CyPA (Abcam, R&D Systems), or IgG controls overnight at 4°C. The proximity ligation assay was further performed according to the manufacturer's instructions. Images were taken on a ZEISS LSM 900 or 980 with Airyscan 2 and a Nikon ECLIPSE Ti2-A and analysed using Fiji/ImageJ.

### 2.6 dSTORM microscopy and structured illumination microscopy

Murine platelets were isolated as previously described<sup>39</sup> and rested in 2 M glycine (AppliChem) coated 8x-well chambers (Cellvis, #C8-1.5H-N, #1.5 high-performance cover glass) for 30 min, before being fixed with 3% glyoxal solution, quenched with 0.1% NaBH<sub>4</sub> (ICN Biomedicals), permeabilized with 0.25% Triton X-100 (Electran), and blocked in a 5% bovine serum albumin (BSA) solution in PBS. Platelets were stained with Alexa Fluor 647-coupled anti-CyPA antibody (R&D Systems) and CF568-coupled anti-RAGE antibody (Abcam) for dSTORM and additionally with MemBrite-488 for structured illumination microscopy. Single- and two-colour dSTORM and the neighbour analysis were performed as previously described.<sup>40</sup> Lattice SIM measurements were performed using a Zeiss Elyra 7 with Lattice SIM<sup>2</sup> equipped with an x63 oil immersion (Plan-Apochromat 63x/1.4 Oil DIC M27) objective and two sCMOS PCO Edge 4.2M cameras. Resting platelets were immobilized using fibrinogen (Sigma-Aldrich) coated 8x-well chambers [Cellvis, #C8-1.5H-N, #1.5 high-performance cover glass (0.170 ± 0.005 mm)]. For Alexa Fluor 647 excitation, the 642 nm laser line (HR Diode 642 nm—500 mW) was used with 10% laser intensity. CF568 was excited with the 561 nm laser line (561 nm DPSS) with 10% laser intensity. The 488 nm laser line (HR Diode 488 nm—500 mW) was used to excite MemBrite-488 as well as Alexa Fluor 488 with 5% laser intensity and 20% laser intensity, respectively. To minimize bleed-through BP 420-480 + LP 655, BP 495-550 + BP 570-620 and BP 420-480 + BP 490-25 + LP 655 filters were used to measure the 642, 561 and 488 nm channels, respectively. In order to align the different channels, a matrix was created using fluorescent beads (TetraSpeck, Thermo Fisher). The channel alignment and SIM<sup>2</sup> image processing were performed using the Zeiss software ZEN 3.0 (black edition). Further image processing/editing was performed using ImageJ.

### 2.7 In silico protein complex modelling

The experimental structures of studied proteins were obtained from the RCSB database (PDB IDs: 7ABT/CyPA,<sup>41</sup> 4YBH/RAGE<sup>42</sup>). Structures were processed with the protein preparation wizard of Schrodinger Maestro suite 2023-2 (Schrodinger Release 2023-2) to optimize the hydrogen-bonding network, followed by constrained minimization (heavy-atom root-mean-square deviation converge of 0.3 Å) to remove crystallographic artefacts. Protein docking was carried out using the Glide<sup>43</sup> protein docking procedure. The docking pose visualized is with lowest (best) Glide docking score value, which is also almost identical to the 4YBH complex.

### 2.8 CyPA-RAGE binding enzyme-linked immunosorbent assay

Interaction of CyPA and RAGE was assessed using a titration enzyme-linked immunosorbent assay (ELISA;  $n \geq 3$ ), as previously described.<sup>44</sup> Wells were coated with recombinant RAGE-Fc, Fc, or CyPA (all R&D Systems) and blocked with 1% BSA for 1 h. CyPA, Fc, or RAGE-Fc was diluted in

HEPES-buffered saline and added for 90 min, respectively, supplemented with 2 mM MgCl<sub>2</sub> and subsequently washed three times. Bound proteins were fixed using 2.5% glutaraldehyde for 10 min. Bound proteins were detected by incubating the plate with an anti-CyPA (Abcam) or anti-Fc (R&D Systems) antibody for 90 min. After washing three times, the plate was incubated with biotinylated secondary antibodies and streptavidin-horseradish peroxidase (HRP). The binding was detected with 3,3',5,5'-tetramethylbenzidine and stopped with 1 M H<sub>2</sub>SO<sub>4</sub>, and the plate was measured at 450 nm.

## 2.9 Immunoprecipitation, siRNA knockdown, and western blot

For immunoprecipitation, HEK293 cells transfected with plasmids pCMV3-AGER-t1-His for RAGE-6xHis and pCMV3-PPIA-GFPspark for CyPA-GFP (Sino Biological) or wild-type platelets were used. Single and co-transfection of HEK293 cells was conducted according to the manufacturer's instructions using Lipofectamine 2000 (Invitrogen). Using the selection marker hygromycin B (0.25 mg/mL, Thermo Fisher), the CyPA-GFP and RAGE-6xHis positive cells were selected. Untransfected and transfected HEK293 cells or platelets after incubation with 100 nM CyPA for 10 min were lysed using radioimmunoprecipitation assay lysis buffer with added protease inhibitor and sonicated subsequently. For immunoprecipitation, the cell lysate was incubated with precipitation antibodies against 6xHis-tag (Abcam), GFPspark-tag (R&D Systems), CD147 (Thermo Fisher), or IgG controls (R&D Systems) overnight at 4°C. The lysate-antibody mix was incubated with agarose bead slurry (Cell Signaling) at 4°C. Afterwards, samples were washed with lysis buffer to remove unbound proteins. The addition of loading dye and dithiothreitol to the bead-bound antibodies and proteins was followed by immunoblot analysis of the samples. Therefore, lysates were separated by sodium dodecyl sulphate-polyacrylamide gel electrophoresis (SDS-PAGE, 10 or 15%) under reducing conditions and transferred onto a polyvinylidene difluoride membrane (PVDF membrane). For detection, primary antibodies against RAGE (Abcam), CD147 (Thermo Fisher), GFPspark-tag, and CyPA (both R&D Systems) with IRDye secondary antibodies (Li-Cor) were used. A Li-Cor Odyssey 9120 System was used for fluorescence signal detection, and representative blots from  $\geq 3$  experiments are shown.

For the detection of RAGE and CD147 in leucocytes, cells were isolated as described above and were treated with anti-CD147 (20  $\mu$ g/mL, Ancell) or SP8356 (10  $\mu$ M, MCE), or respective controls for the indicated time periods. For siRNA knockdown, THP-1 cells were transfected using Accel transfection medium (Horizon Discovery) with siRNA targeting RAGE, CD147, or non-targeted control RNA (1  $\mu$ M, Horizon Discovery). Western blot of leucocyte or platelet lysates was performed according to standard protocols using anti-CD147 (Thermo Fisher) or anti-RAGE (Abcam) antibodies for detection.

## 2.10 RAGE-CHO cells

RAGE-CHO and respective parental cells were cultured in Ham's-F12 Medium supplemented with 10% foetal calf serum and 1% Na pyruvate. For western blots, cells were lysed in lysis buffer with protease inhibitor (both Cell Signaling) for 1 h at 4°C. A 5 $\times$  sample buffer was added, and samples were kept for 5 min at 95°C. The samples were run on 8.5% SDS-polyacrylamide gels. For RAGE detection, anti-RAGE antibody (Santa Cruz), diluted in 5% BSA, was used. Bands were detected using a Li-Cor Odyssey 9120 infra-red imaging system (Li-Cor). Verification of surface expression of RAGE was done by flow cytometry. Flow cytometry also confirmed that RAGE-CHO cells did not differ in their CD147 expression from CHO cells. Adhesion experiments ( $n \geq 8$ ) under flow were performed as described before.<sup>45</sup>

## 2.11 Atomic force microscopy

To investigate the interaction of CyPA with RAGE expressed on the cell surface, we used atomic force microscopy to evaluate minute differences in binding strength between RAGE and CyPA. CHO and RAGE-CHO cells were kept in fibronectin-coated wells in Leibovitz's L-15 Medium (Thermo

Fisher). Force measurements between a CyPA-coated cantilever (MLCT-BIO-DC, cantilever C,  $k \approx 0.01$  N/m, Bruker Corporation) and the cell surface of CHO ( $n = 75$ ) and RAGE-CHO ( $n = 78$ ) cells were obtained using an MFP3D-BIO atomic force microscope (Asylum Research) in the force mapping mode with the following scan parameters: trigger: 1 nN, retract distance: 4  $\mu$ m, contact dwell time: 2 s, force curve rate: 1–2 Hz, and scan size: 5  $\times$  5  $\mu$ m<sup>2</sup> and 6  $\times$  6 pixels, resulting in 36 adhesion measurements per cell; per condition, more than 76 cells were analysed from two individual experiments. Analyses were performed using IGOR PRO 8 (WaveMetrics).

## 2.12 Chemotaxis of monocytes and leucocytes

The migration of human monocytes and murine leucocytes was assessed using a modified Boyden chamber (Neuro Probe).<sup>4</sup> For human monocytes, a 5  $\mu$ m and, for murine leucocytes, a 3  $\mu$ m pore polycarbonate membrane was used to separate the upper and the lower compartment; 2  $\times$  10<sup>4</sup> cells/well were loaded in the upper chamber in the presence or absence of the receptor blocking antibodies anti-CD147 (Ancell), anti-RAGE (Abcam, R&D Systems), anti-TLR4 (R&D Systems), or IgG control (all 20  $\mu$ g/mL). CyPA (200 nM) or CXCL12 (50  $\mu$ g/mL, both R&D Systems) was added to the medium in the lower chamber as specified. For decoy receptor experiments, CyPA was preincubated with recombinant RAGE-Fc or Fc (3.6  $\mu$ g/mL, respectively, both R&D Systems). After migration for 4 h at 37°C with a 5% CO<sub>2</sub> atmosphere, the separating membrane was fixed with methanol and the cells were stained with a May-Grünwald/Giemsa solution and counted.

## 2.13 Static adhesion

Static adhesion was assessed using CyPA- or BSA-coated wells. Leucocytes from *Ager*<sup>-/-</sup> or wild-type mice or human monocytes were preincubated with anti-RAGE, anti-CD147, anti-RAGE, and anti-CD147, or IgG control (all 20  $\mu$ g/mL) for 15 min; 2  $\times$  10<sup>4</sup> cells were allowed to adhere to immobilized CyPA or BSA for 1 h. Hereafter, the plate was gently washed to remove non-adherent cells and adherent cells were counted.

## 2.14 Dynamic adhesion

Flow chamber experiments with leucocytes were performed as previously described.<sup>17,45</sup> In brief, cover slips were coated with recombinant CyPA, BSA, or human umbilical vein endothelial cells (HUVECs) in the presence or absence of 800 nM MM284, an extracellular cyclosporine derivative blocking extracellular CyPA, where indicated. LPS- or CyPA-stimulated human monocytes, CyPA-stimulated leucocytes from *Ager*<sup>-/-</sup> or wild-type mice (2  $\times$  10<sup>5</sup>), or (RAGE-)CHO cells were used and were preincubated with either anti-RAGE (R&D Systems) or anti-CD147 (Ancell) antibody or IgG control (all 20  $\mu$ g/mL) where indicated and were perfused over recombinant CyPA or activated HUVECs under arterial shear rates of 2000 s<sup>-1</sup>. The experiments were recorded in real time, and rolling and adherent cells were evaluated off-line.

## 2.15 MyD88 activation

The 4  $\times$  10<sup>4</sup> THP-1 cells were pretreated for 15 min with either SP8356 (10  $\mu$ M, MCE) or anti-CD147 (20  $\mu$ g/mL, Ancell) to block CD147. RAP or FPS-ZM1 (300 nM, Merck) was used to block RAGE. IgG or the respective solvent was used as negative control. Cells were activated by LPS (1  $\mu$ g/mL) as a positive control or CyPA (200 nM, R&D Systems) for 8 min alone or following the antagonist pretreatment. Cells were fixed in 4% paraformaldehyde (PFA) for 10 min, washed, and permeabilized for 15 min with PBS containing 5% BSA and 0.3% Triton X-100. Primary anti-MyD88 antibody (Santa Cruz) was diluted 1:50 in PBS, and cells were incubated for 1 h. The secondary antibody donkey anti-goat Alexa 488 (Life Technologies) was incubated 1 h in the dark. Nuclei were stained with Draq5 (Thermo Scientific). Between each step, cells were thoroughly washed three times with PBS. Slides were mounted with Prolong Diamond Antifade (Invitrogen). MyD88 activation was assessed

in cells visualized using a Nikon Eclipse Ti2-A microscope at  $\times 60$  using 660 and 495 nm filters.

## 2.16 NF- $\kappa$ B translocation

Human leucocytes were isolated and cultivated in RPMI 10% FBS at 37°C with 5% CO<sub>2</sub> overnight. Cells were pretreated for 15 min with either SP8356 (10  $\mu$ M, MCE), anti-CD147 (20  $\mu$ g/mL, Ancell), RAP, or FPS-ZM1 (both 300 nM, Merck), or with the respective solvent or IgG as negative control. Cells were activated for 30 min with either LPS (1  $\mu$ g/mL) as a positive control or CyPA (200 nM, R&D Systems). For immunofluorescence measurements, *in situ* cells were fixed in 4% PFA for 10 min and, after a PBS wash step, permeabilized 15 min with PBS, 5% BSA, 0.3% Triton X-100 (PB). Cells were incubated for 1 h with rabbit-anti-NF- $\kappa$ B p65 (Cell Signaling) 1:400 in PB. Secondary donkey anti-rabbit Alexa 488 antibody (Life Technologies) was incubated for 1 h in the dark. Nuclei were stained with Draq5 (Thermo Scientific). Slides were mounted with Prolong Diamond Antifade (Invitrogen) and visualized with a Nikon Eclipse Ti2 microscope at  $\times 60$ . Images of nuclei (660 nm) and NF- $\kappa$ B staining (495 nm) were taken and fluorescence intensity in the nucleus was assessed using ImageJ.

For electrophoretic mobility shift assay (EMSA), nucleus extracts of the cells were prepared as previously described.<sup>46</sup> The Odyssey infra-red EMSA assay kit (Li-Cor) was performed according to the manufacturer's recommendations using IRDye 700 NF- $\kappa$ B consensus oligonucleotide as well as 200 $\times$  unlabelled oligonucleotides. Gels were imaged using a Li-Cor Odyssey 9120 imaging system.

## 2.17 Intravital microscopy of postcapillary venules in murine cremaster muscle

To study leucocyte rolling *in vivo*, postcapillary venules of the mouse cremaster muscle were visualized, as described.<sup>28</sup> Two hours after intrascrotal injection of 10  $\mu$ g CyPA or PBS, anaesthesia was induced by intraperitoneal injection of ketamine and xylazine (100/20 mg per kg body weight, respectively), and a tracheal tube was inserted for ventilation. The scrotum was opened and the cremaster muscle was exteriorized. By spreading it over a cover glass and superfusing it with bicarbonate-buffered saline (35°C), the postcapillary venules were visualized using an upright Olympus BX51 microscope with a saline immersion objective ( $\times 40/0.8$ ). Data were analysed offline on stored video tracks. Diameters and length of postcapillary venules were analysed using a digital image processing system.<sup>47</sup> The centreline red blood cell velocity was determined with a dual photodiode with a digital on-line cross-correlation program (Circusoft Instrumentation) for off-line calculation of the mean blood flow velocity and shear rates.<sup>48</sup> The number of adherent leucocytes, defined as cells that remain stationary at the vessel wall during a 30-s observation period, per vessel surface (n/mm<sup>2</sup>) and rolling leucocyte flux fraction, defined as the number of rolling cells crossing a perpendicular line through the examined vessel during 1 min in relation to the total number of circulating leucocytes, were calculated.

## 2.18 Induction of peritonitis *in vivo*

Eight- to twelve-week-old wild-type and RAGE-deficient *Ager*<sup>-/-</sup> mice were intraperitoneally injected with 10  $\mu$ g CyPA. After 24 and 48 h, mice were sacrificed and a peritoneal lavage was performed by washing the peritoneum with PBS. After 24 h, one mouse of each group had to be excluded from analysis due to haemorrhagic lavage, which was a prespecified exclusion criterion. The infiltrated cells were harvested, and  $5 \times 10^5$  cells were stained for the surface markers CD11b, F4/80, and CD3 (all eBioscience) and analysed by flow cytometry.

## 2.19 Flow cytometry analysis of murine leucocytes

Eight- to twelve-week-old C57BL/6 mice were injected i.p. with the anti-CyPA antibody 8H7 or IgG control (5  $\mu$ g/kg). After 24 h, mice were sacrificed and blood was collected in PBS supplemented with 20 U heparin. Erythrocytes were lysed twice using lysis buffer

(155 mM NH<sub>4</sub>Cl, 12 mM NaHCO<sub>3</sub>, and 0.1 mM EDTA in ddH<sub>2</sub>O, pH 7.2–7.6). Cells were washed, supernatant was discarded, and cells were blocked (TruStain FcX anti-mouse CD16/32, Biolegend and NovaBloc, Invitrogen). Cells were stained with antibodies against CD3, CD4, CD8 (all BD Bioscience), CD25 (BioLegend), CD11b (Miltenyi Biotec), RAGE (R&D Systems), and anti-FoxP3 (Thermo Fisher), or CD147 for 20 min. Hereafter, cells were washed twice, fixed, and permeabilized overnight at 4°C with FoxP3 Staining Buffer Set (eBioscience) according to manufacturer's instructions and analysed using a Cytex Aurora.

## 2.20 Platelet isolation and flow cytometry analysis

Human platelets were isolated as previously described.<sup>17,49</sup> In brief, blood was drawn in CPDA monovettes (Sarstedt) and centrifuged to obtain platelet-rich plasma (PRP). Murine platelets were isolated using acid citrate dextrose. Platelets were stimulated for 1 h with 200 nM CyPA together with 20  $\mu$ g/mL anti-RAGE, IgG control or adenosine diphosphate (ADP, 20  $\mu$ M), or thrombin (1 U/mL) in Tyrode's HEPES buffer supplemented with 1 mM CaCl<sub>2</sub>. The platelets were stained for CD29, CD41a, CD49b, CD147 (all BioLegend), CD62P (human: Beckman Coulter; murine: Emfret Analytics), CD42b, and/or JON/A (both Emfret Analytics) and analysed by flow cytometry.

Aggregation of CD14<sup>+</sup> cells with platelets was assessed as previously described.<sup>18</sup> In brief, isolated platelets ( $1 \times 10^7$ ) were stimulated with CyPA (200 nM) or TRAP (25  $\mu$ M) and incubated with anti-RAGE, anti-CD147, both, or IgG control (all 20  $\mu$ g/mL) for 30 min. Activated platelets were incubated with isolated leucocytes ( $5 \times 10^5$ ) for 1 h and were stained with anti-CD14 (R&D Systems) and anti-CD42b (BD Biosciences). Double-positive co-aggregates were analysed by flow cytometry.

## 2.21 Calcium measurements

Washed human platelets were resuspended in Tyrode's buffer without calcium and loaded with 5  $\mu$ M fura-2 acetoxymethyl ester (Invitrogen) in the presence of 0.2  $\mu$ g/mL Pluronic F-127 (Biotium) for 30 min at 37°C. Loaded platelets, washed once and resuspended in Tyrode's buffer containing 1 mM Ca<sup>2+</sup>, were treated with CyPA (200 nM) or solvent control (PBS) for 10 min and subsequently activated with ADP (20  $\mu$ M) in the presence or absence of FPS-ZM1 (400 nM, Merck). Calcium responses were measured under stirring with a spectrofluorometer (LS55, PerkinElmer), at alternate excitation wavelengths of 340 and 380 nm (37°C). The 340/380 nm ratio values were converted into nanomolar concentrations of Ca<sup>2+</sup> by lysis with Triton X-100 (Sigma-Aldrich) and a surplus of EGTA.

## 2.22 *In vitro* thrombus formation

*In vitro* thrombus formation was performed as previously described.<sup>17,49</sup> Glass cover slips were coated with collagen and blocked for 1 h with 1% BSA. Human CPDA-anticoagulated blood or murine-heparinized blood was stimulated with 200 nM CyPA for 1 h or kept in resting conditions. The blood was additionally pretreated for 15 min with antibodies against CD147, RAGE, CD147 and RAGE, or IgG control (all 20  $\mu$ g/mL). The blood was perfused over cover slips with a shear rate of 1000 s<sup>-1</sup>. Photo documentation for analysis was performed after blood perfusion was stopped. The thrombus area was analysed off-line, and the relative thrombus area was calculated.

## 2.23 Statistical analysis

Data are presented as mean  $\pm$  SEM. Normality was assessed and Student's *t*-test or non-parametric tests were used for comparisons between two groups. Comparisons between more than two groups were performed using analysis of variance (ANOVA) or Kruskal–Wallis test with subsequent *post hoc* two-stage linear step-up procedure of Benjamini, Krieger, and Yekutieli. The analyses were performed using GraphPad Prism (GraphPad Software). A *P* < 0.05 was considered statistically significant. ns indicates *P* > 0.05, \*

indicates  $P < 0.05$ , \*\* indicates  $P < 0.01$ , \*\*\* indicates  $P < 0.001$ , and \*\*\*\* indicates  $P < 0.0001$ .

## 3. Results

### 3.1 RAGE interacts with CyPA on the cell membrane

To investigate whether RAGE can interact with extracellular CyPA, we first compared the localization of RAGE with the well-characterized CyPA receptor CD147 on human leucocytes. Confocal microscopy revealed similar distribution of RAGE when comparing it to the localization of CD147, both being predominantly found at the cell membrane (Figure 1A). CyPA was furthermore found closely associated with CD147 as well as with RAGE on the cell surface. Using proximity ligation for CyPA and RAGE, we observed a robust colocalization signal on human leucocytes *in situ* (Figure 1B and C). When RAGE was targeted with the small-molecule inhibitor FPS-ZM1<sup>50</sup> or RAP,<sup>51</sup> we observed a marked decrease in signal strength (Figure 1B, bottom panel). Leucocytes from *Ager*<sup>-/-</sup> mice similarly showed no specific PLA signal compared to leucocytes from wild-type mice (Figure 1C). These findings indicate that CyPA interacts in close proximity with RAGE and that inhibition of RAGE prevents this association on the cell surface.

We further used super resolution microscopy technology with two-colour dSTORM in conjunction with lattice structured illumination microscopy (Figure 1D and E) to investigate the CyPA–RAGE interaction in murine platelets after verifying that RAGE is expressed on human platelets (see Supplementary material online, Figure S1A). Neighbour density analysis showed accumulation of RAGE in close proximity to CyPA in the range of 50–100 nm on a single-molecule level. When taking into account that the two antibodies used for staining induce distance errors of 10–15 nm each, these analyses allow for a very exact determination of spatial congruency between the two molecules.

*In silico* protein complex modelling of the CyPA–RAGE interaction confirmed a suspected binding site between the two molecules with the lowest (best) Glide docking value shown, being almost identical to the RAGE complex (Figure 2A). In the next step, we used a CyPA–RAGE-binding ELISA to investigate binding of the two interaction partners in the absence of other proteins to confirm that CyPA and RAGE interact with each other in the absence of other facilitating factors. We observed a significant binding between RAGE-Fc and plate-bound CyPA and *vice versa* compared to the Fc control (Figure 2B). The concentration of RAGE required for half-maximal CyPA binding was found to be in the range of 2–5 µg/mL.

Using co-immunoprecipitation, we confirmed the CyPA–RAGE interaction by generating plasmids coding for tagged CyPA or RAGE, which were transfected in HEK293 cells. Expression was verified by immunofluorescence microscopy (not shown). We found that immunoprecipitation of CyPA from cells transfected with CyPA-GFP showed a positive immunoreactive band for RAGE. Further, immunoprecipitation of RAGE (RAGE-HIS) showed a positive immunoreactive band for CyPA (CyPA-GFP) in transfected cells. Interaction of CyPA with the known receptor CD147 was confirmed by detecting CD147 after immunoprecipitation of CyPA-GFP and the detection of CyPA after immunoprecipitation of CD147 (Figure 2C).

To further differentiate a mere spatial association from a significant and strong binding of the two proteins on the cell surface, we performed atomic force microscopy (Figure 2D, top).<sup>52</sup> We used RAGE-expressing CHO cells showing a markedly increased surface expression of RAGE while retaining a similar CD147 surface expression compared to the parental cells (Figure 2E). We measured the adhesion force and adhesion work required to remove a CyPA-coated cantilever from the cell surface of RAGE CHO and CHO cells, respectively (Figure 2D, bottom). RAGE CHO cells elicited a strongly increased adhesion force and adhesion work necessary to lift the cantilever from the cell surface compared to the parental cell, which illustrates a significant and strong CyPA–RAGE interaction on the cell surface, which goes beyond a spatial association.

RAGE has been described to be released from cells [soluble RAGE (sRAGE)] and to act as a decoy receptor modifying its ligands by binding

them in the extracellular space before they reach a surface-associated RAGE molecule, thereby proving a sink for proinflammatory ligands.<sup>53,54</sup> We observed that human monocytes readily migrate towards extracellular CyPA in the absence of sRAGE. However, the pro-migratory effect of CyPA was mitigated by preincubation with sRAGE mimicking the biological function of sRAGE (Figure 2F). This provides additional clues about the dynamic ligand receptor interactions beyond the cell surface.

RAGE-CHO cells furthermore displayed increased rolling when perfused over CyPA-coated surfaces compared to the parental cells. This was abolished when the CyPA-coated surface was preincubated with MM284, a cell-impermeable cyclosporine derivative, which selectively binds extracellular CyPA (Figure 2G).

### 3.2 RAGE is necessary for CyPA-induced signalling via MyD88 and NF-κB in leucocytes

We further examined the role of RAGE and CD147-induced signalling events in response to extracellular CyPA. We first investigated the activation of MyD88, a 296 amino acid downstream adaptor protein of RAGE, which shows no known association with CD147.<sup>21</sup> When THP-1 cells were challenged with extracellular CyPA, we observed a robust increase in MyDosome activation, which was comparable to stimulation with LPS. To our surprise, this effect was blunted when RAGE or CD147 was inhibited by antibody or small-molecule inhibitors (RAGE inhibitors FPS-ZM1 and RAP; CD147 inhibitor SP8356, Figure 3A). This indicates that RAGE in addition to CD147 is a significant interaction partner for extracellular CyPA, and that both receptors seem to be necessary for efficient signal transduction to activate MyD88. Functionally, MyD88 activation was required for CyPA-induced cell migration. Leucocytes from *Myd88*<sup>-/-</sup> mice showed a significantly reduced migration towards extracellular CyPA compared to wild type, whereas migration towards CXCL12 (SDF1), which induces migration by binding to CXCR4/CXCR7, was unaltered, showing that *Myd88*-deficient leucocytes have no general migration deficiency (Figure 3B).

We found striking parallels in the activation of NF-κB in human leucocytes. Here, CyPA induced a translocation of NF-κB into the nucleus, comparable to LPS used as positive control. Inhibition of RAGE or CD147 resulted in a similarly decreased NF-κB translocation when evaluating nuclear fluorescence signal of NF-κB p65 *in situ* (Figure 3C), which was verified by EMSA of NF-κB performed with nuclear protein extracts (Figure 3D). Taken together, these results indicate an intricate dependence of CyPA, both on RAGE and CD147.

### 3.3 RAGE is necessary for CyPA-induced recruitment of leucocytes

We were furthermore interested to determine the role of RAGE for CyPA-induced leucocyte recruitment. We first analysed the adherence of human monocytes to immobilized CyPA in a static adhesion model. We found monocytes to strongly adhere to immobilized CyPA, while antibody-based inhibition of the receptors CD147, RAGE, or both significantly reduced adhesion (Figure 4A). Monocyte adhesion under dynamic conditions was investigated using a flow chamber assay with arterial shear rates, which imposes physical stress on the facilitating proteins on the surfaces. When human monocytes were perfused over a CyPA-coated surface, the addition of anti-RAGE antibody diminished the CyPA-induced adhesion markedly, as did the addition of anti-CD147 antibody (Figure 4B). A similar effect was observed by perfusing CyPA-stimulated human monocytes over activated HUVECs, where adhesion was significantly reduced upon the addition of anti-CD147 or anti-RAGE antibody (Figure 4C). A simultaneous inhibition of CD147 and RAGE did not result in a further reduction of the already low adhesion (Figure 4C).

To assess whether RAGE is involved in CyPA-induced chemotaxis of leucocytes, a modified Boyden chamber assay was used. The addition of anti-RAGE antibody significantly abrogated the chemotactic response of human leucocytes towards extracellular CyPA (Figure 4D). Similarly, a

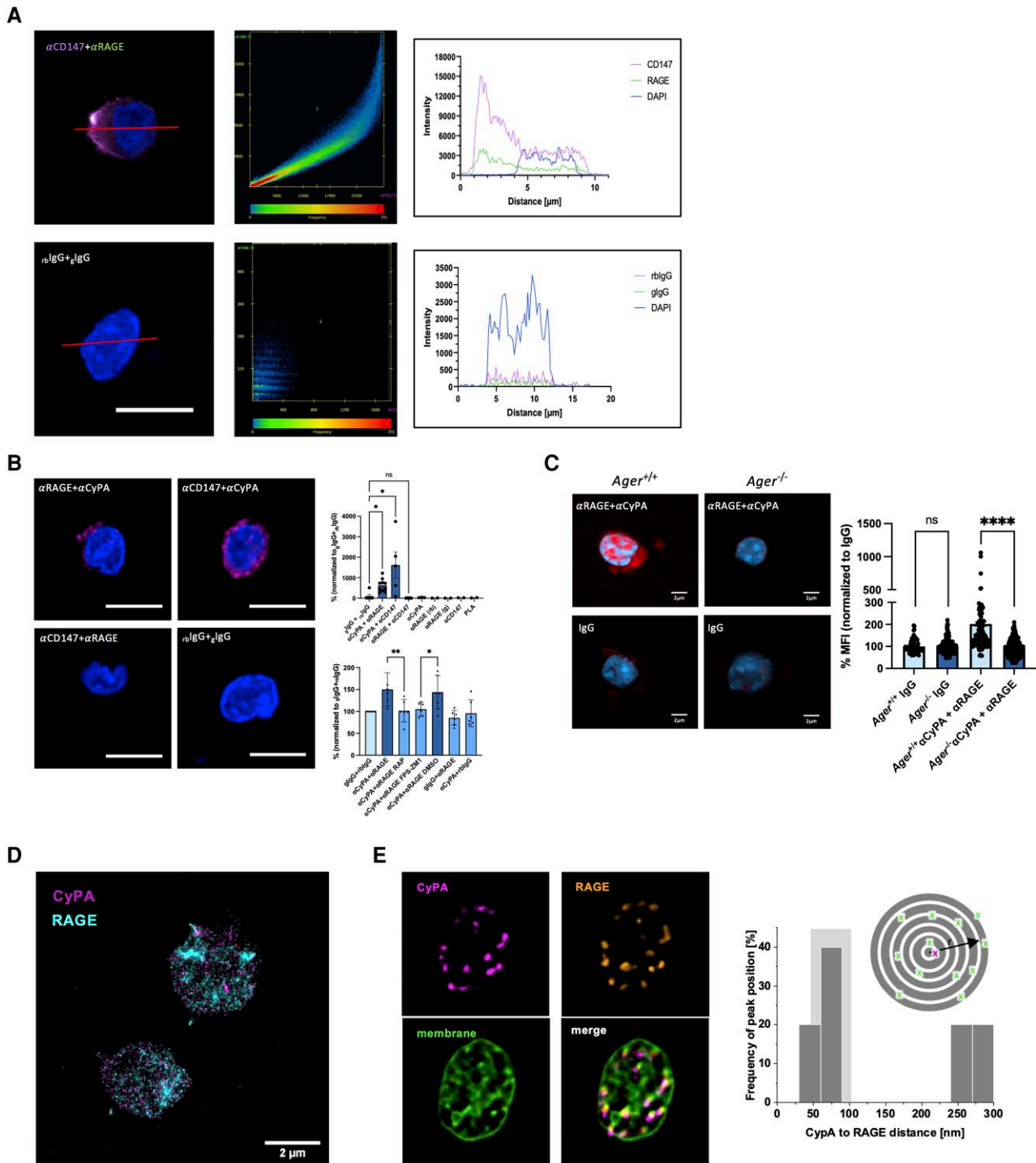


**Figure 1** CyPA interacts with RAGE and CD147 on leucocytes and platelets. Confocal single plane images of human monocytes stained with antibodies against RAGE and CD147 showed a similar cellular distribution of the two receptors (left panel). Colocalization analysis (centre panel) demonstrated a strong signal overlap between the two receptors. Spatial signal analysis along the red line highlights the strongest signal overlap in the area of the cell membrane (A, right panel; scale bar 5  $\mu$ m). Proximity ligation assays (PLA) on human leucocytes furthermore confirmed a close spatial interaction of CyPA with RAGE and CD147, while CD147 and RAGE display no close interaction. This interaction of CyPA with RAGE was blocked by addition of the RAGE inhibitors FPS-ZM1 and RAP (B, top panel  $n \geq 2$  biological replicates, Kruskal–Wallis test bottom panel  $n = 6$  biological replicates, ANOVA, scale bar 5  $\mu$ m). Leucocytes from *Ager*<sup>-/-</sup> mice similarly showed no specific PLA signal compared to *Ager*<sup>+/+</sup> mice (C,  $n = 4$  biological replicates, Mann–Whitney test, scale bar 2  $\mu$ m). Super-resolution microscopy of murine platelets (D, two-colour dSTORM; E, Lattice SIM) confirmed colocalization of CyPA and RAGE. Neighbour density analysis of RAGE density in discrete ring areas (dark grey) in relation to CyPA allowed identification of colocalization hotspots through analysis of RAGE density at different radial distances to CyPA. Histograms of distance-dependent density peak maxima in resting platelets with increased accumulation distances as indications of colocalization hotspots highlighted in light grey between 50 and 100 nm are shown (scale bar 2  $\mu$ m). \* indicates  $P < 0.05$ , \*\* indicates  $P < 0.01$ , \*\*\*\* indicates  $P < 0.0001$ , and ns indicates  $P > 0.05$ .

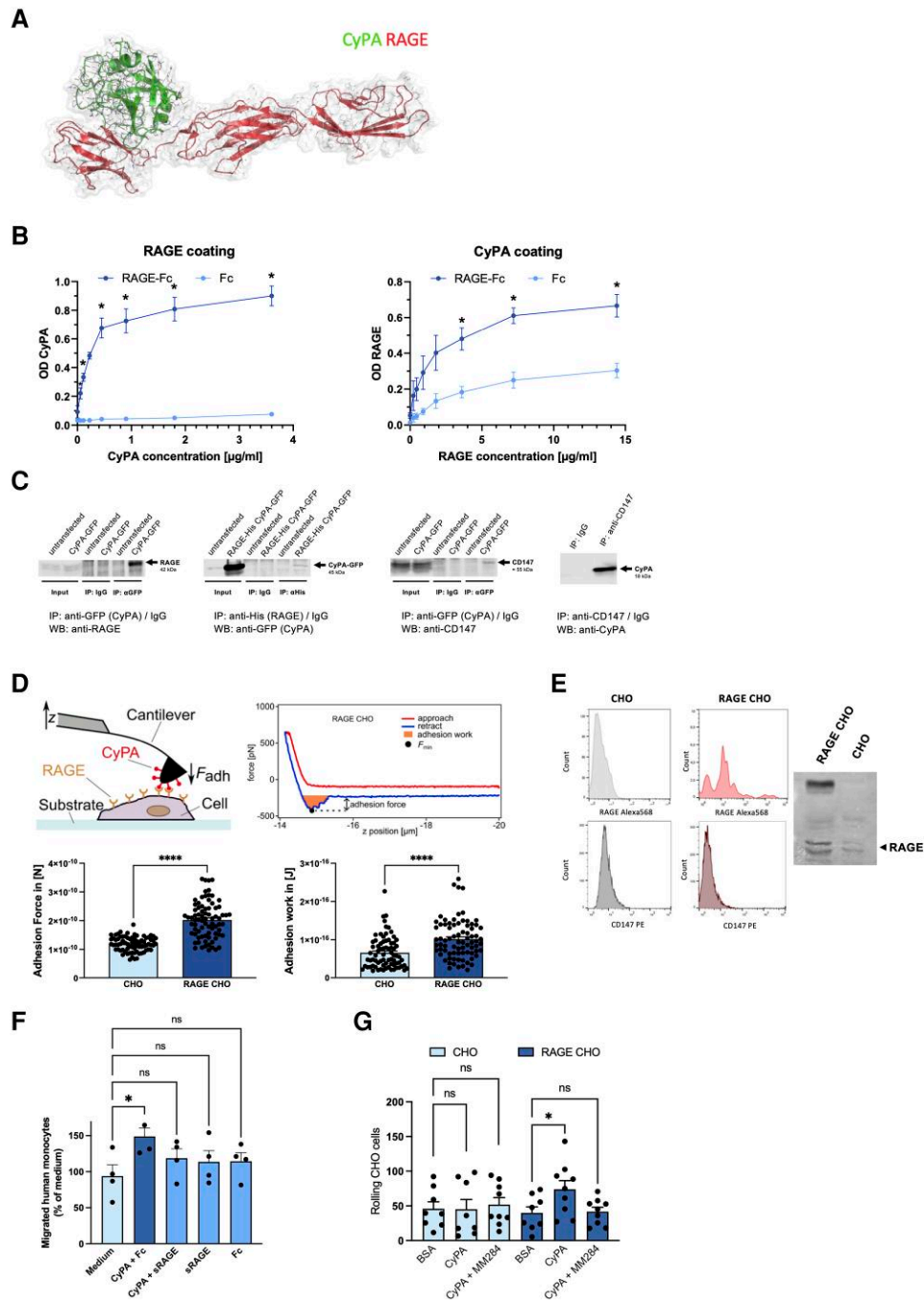


**Figure 2** CyPA is bound by RAGE on the cell surface. To evaluate binding sites, *in silico* protein complex modelling was performed between CyPA and RAGE. Protein docking was carried out using the Glide protein docking procedure. The docking pose with the lowest (best) Glide docking score value is visualized and is also almost identical to the RAGE complex and is shared by several other known RAGE ligands (A). ELISAs of recombinant RAGE-Fc to CyPA showed a significant interaction of the two proteins in a dose-dependent manner (B,  $n \geq 3$  biological replicates, *t*-test). Immunoprecipitations from HEK293 cells transfected with CyPA-GFP and/or RAGE-HIS, or platelets (right panel), show an interaction of CyPA with RAGE and CD147. Representative micrographs of blots are shown (C,  $n \geq 3$  biological replicates). Atomic force microscopy was used to characterize the CyPA–RAGE interaction on the cell surface. Adhesion of a CyPA-coated cantilever was significantly higher on RAGE-transfected CHO cells compared to parental cells, while CD147 surface expression was similar in both cell types, as shown by FACS. RAGE expression in CHO and RAGE-CHO cells was confirmed by western blot and FACS (D, E, individual dots show mean of 36 measurements per cell;  $n \geq 76$  cells were analysed per condition, *t*-test, Mann–Whitney test). Migration of human leucocytes towards CyPA was blocked by preincubation of CyPA with recombinant RAGE or Fc as control (both 3.6  $\mu\text{g}/\text{mL}$ ), mimicking the ability of sRAGE to modulate its ligands before binding to membrane-bound RAGE, abrogating subsequent signalling *in vivo* (F,  $n \geq 3$  biological replicates, ANOVA). RAGE-CHO cells showed increased rolling on CyPA-coated surfaces under flow conditions compared to non-transfected parental cells. Preincubation of CyPA with the CyPA-binding extracellular cyclosporine derivative MM284 (800 nM) blocked this effect (G,  $n \geq 8$  biological replicates, ANOVA). \* indicates  $P < 0.05$ , \*\*\*\* indicates  $P < 0.0001$ , and ns indicates  $P > 0.05$ .



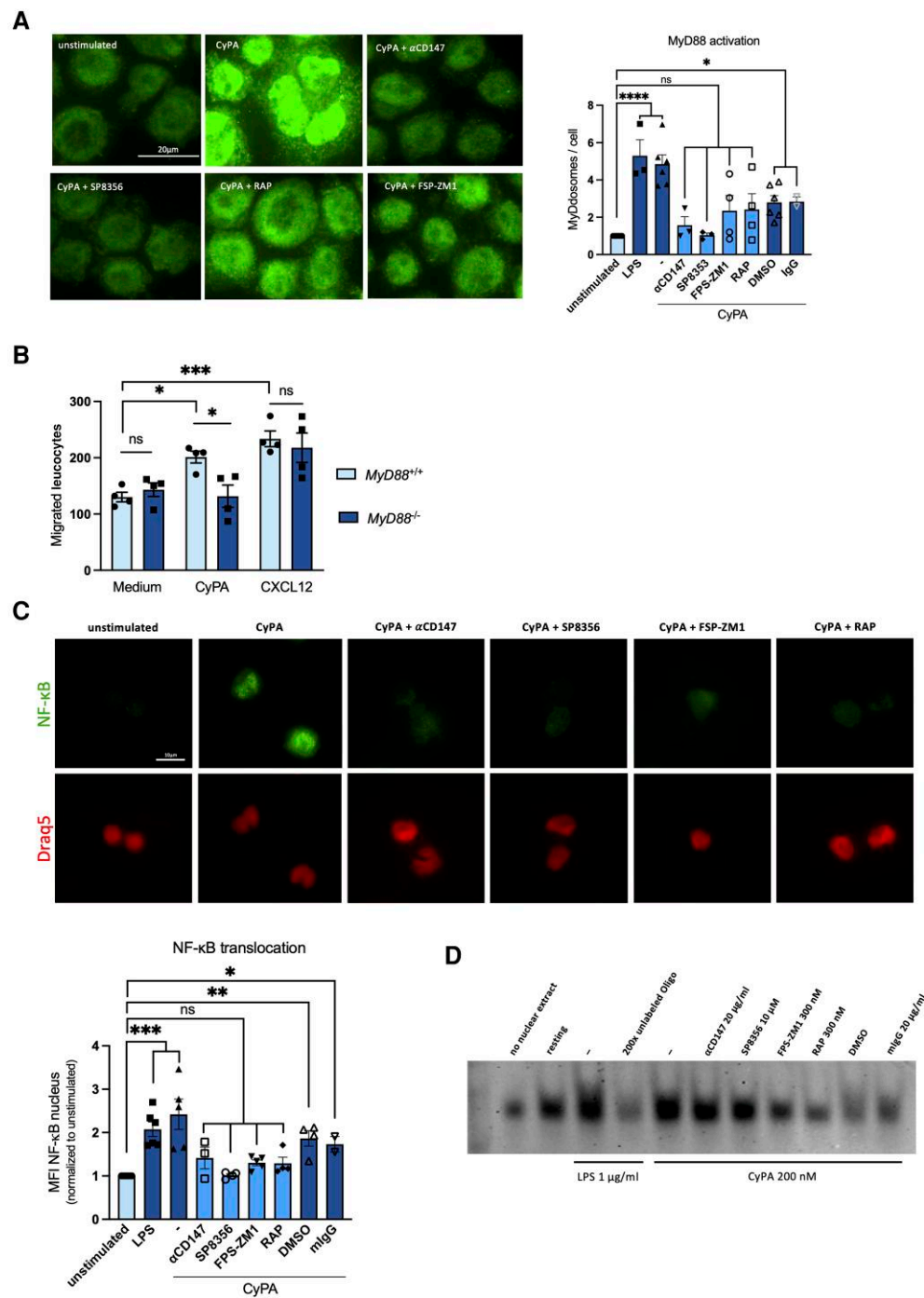


**Figure 3** RAGE is necessary to activate downstream signalling upon CyPA stimulation. Stimulation of THP-1 cells with CyPA (200 nM) resulted in a strong activation of MyD88. This was diminished when RAGE was blocked using the inhibitors FPS-ZM1 or RAP (both 300 nM). Similarly, activation was reduced by blocking CD147 with the inhibitor SP8356 (10 μM) or anti-CD147 antibody (20 μg/mL; A,  $n \geq 3$  biological replicates, ANOVA). Consistently, leucocytes from MyD88-deficient mice showed no relevant migration towards CyPA (200 nM) compared to leucocytes from wild-type mice, while both showed normal migration towards CXCL12 (50 μg/mL; B,  $n = 4$  biological replicates, ANOVA). Activation and subsequent translocation of NF-κB p65 to the nucleus of human leucocytes was induced by stimulation with CyPA (200 nM), and NF-κB p65 fluorescence signal (green) at the nucleus (Draq5, red) was measured. A reduced translocation of NF-κB p65 was observed when RAGE was blocked with FPS-ZM1 or RAP (both 300 nM), or when CD147 was blocked with SP8356 (10 μM) or anti-CD147 antibody (20 μg/mL; C,  $n \geq 3$  biological replicates, Kruskal–Wallis test). EMSA of nucleus extracts of human leucocytes using fluorescent double-stranded DNA oligonucleotides of NF-κB was used to assess the role of CD147 and RAGE on CyPA-induced NF-κB activation. Blocking of CD147 [preincubated with anti-CD147 (20 μg/mL), SP8356 (10 μM)] or RAGE [preincubated with FPS-ZM1, RAP (both 300 nM)] resulted in a decrease of nuclear binding signal of NF-κB compared to CyPA alone. Addition of 200x unlabelled oligonucleotide resulted in a decreased signal as well, which confirms the specificity of the observed binding signal (D, representative blot of three biological replicates is shown; others are shown in [Supplementary material online, Figure S1B](#)). \* shows  $P < 0.05$ ; \*\* shows  $P < 0.01$ ; \*\*\* shows  $P < 0.001$ ; \*\*\*\* shows  $P < 0.0001$ ; ns shows  $P > 0.05$ .

strong reduction of migration was observed when anti-CD147 antibody was added to the cells, as described before. IgG isotype control and control anti-TLR4 antibody did not interfere with CyPA-induced migration.

We furthermore used leucocytes from *Ager*<sup>-/-</sup> mice to investigate effects of complete disruption of the CyPA–RAGE signalling on cell adhesion and migration. Leucocytes from *Ager*<sup>-/-</sup> mice were verified to have similar CD147 expression levels compared to wild-type mice (Figure 4E). siRNA knockdown of CD147 or RAGE in THP-1 cells did not result in reciprocally altered expression of the respective other receptor compared to untreated cells or cells transfected with control siRNA (Figure 4F).

In a static adhesion assay, a significantly higher binding of wild-type leucocytes to recombinant CyPA compared to BSA control was noted, whereas *Ager*<sup>-/-</sup> leucocytes did not show any relevant adhesion to recombinant CyPA or BSA (Figure 4G). Under flow conditions, *Ager*<sup>-/-</sup> leucocytes showed no relevant rolling on immobilized CyPA compared to cells from wild-type animals (Figure 4H). Furthermore, extracellular CyPA failed to induce migration of *Ager*<sup>-/-</sup> leucocytes, whereas leucocytes from wild-type animals showed normal migration towards CyPA (Figure 4I).

These data indicate that both RAGE and CD147 are required for CyPA-mediated leucocyte recruitment and adhesion.

### 3.4 CyPA-induced leucocyte recruitment is dependent on RAGE *in vivo*

Leucocyte recruitment is a tightly regulated process in which RAGE has been identified to play a prominent role. We were therefore interested, whether CyPA acts via RAGE to induce leucocyte adhesion to the vessel wall also *in vivo*. Hence, we investigated the relevance of the CyPA–RAGE interaction for leucocyte recruitment to the vessel wall using intravital microscopy of the postcapillary venules in the cremaster muscle of mice. Intrascrotal injection of CyPA induced a strong adhesion of leucocytes to the postcapillary venules in wild-type mice. In RAGE-deficient mice, however, CyPA injection resulted in a diminished adhesion of leucocytes similar to injection with PBS, indicating that RAGE is necessary for CyPA-induced recruitment of leucocytes to the vessel wall *in vivo* (Figure 5A).

To evaluate the pathophysiological significance of the CyPA–RAGE interaction for leucocyte chemotaxis to the site of inflammation *in vivo*, we performed a CyPA-induced murine peritonitis model. When wild-type mice were injected with CyPA into the peritoneal cavity, a strong influx of leucocytes was apparent. In contrast, CyPA injection into *Ager*<sup>-/-</sup> mice resulted in a drastically decreased recruitment of leucocytes compared to wild-type mice. The effect was pronounced after 24 h for CD11b-positive and CD3-positive cells while F4/80-positive cells reached statistical significance after 48 h (Figure 5B and C).

### 3.5 CyPA plays an important regulatory role for RAGE expression *in vivo*

To show that not only externally administered CyPA interacts with RAGE in an experimental model, we were interested to investigate whether a positive feedback loop between basal extracellular CyPA as the ligand and the regulation of RAGE as the receptor exists *in vivo*, which has been published for several ligands, both for RAGE and CD147, respectively.<sup>55,56</sup> When wild-type mice were treated with the CyPA-binding antibody 8H7 for 24 h to reduce basal extracellular CyPA levels, we observed a dramatic decrease of RAGE on leucocytes. This was not restricted to one subpopulation but was detected on CD11b<sup>+</sup>, CD4<sup>+</sup>, CD8<sup>+</sup> ( $P < 0.05$ , respectively), and regulatory T cells ( $P = 0.08$ ), indicating an important regulatory role of extracellular CyPA in the expression of RAGE on leucocytes *in vivo* (Figure 5D). These data provide strong evidence that extracellular CyPA indeed is tightly intertwined with RAGE as its receptor in leucocyte recruitment and that CyPA subsequently has an important regulatory role in the expression of RAGE *in vivo*.

## 3.6 CyPA-induced activation and adhesion of platelets are dependent on CyPA–RAGE interaction

CyPA has previously been identified to activate platelets and to serve as a crosslink in thrombo-inflammation.<sup>17</sup> To determine whether the effects of the CyPA–RAGE interaction are limited to leucocytes, we confirmed the expression of RAGE on human platelets (see [Supplementary material online, Figure S1A](#)) and evaluated their role in the activation of human platelets upon CyPA stimulation. In response to the canonical platelet activator ADP, platelets increase surface CD62P expression. Also, in response to CyPA, we noted an increased CD62P expression, which was significantly abrogated when platelets were treated with anti-RAGE antibody prior to CyPA stimulation (Figure 6A). This confirms that RAGE is also a relevant receptor for the activation of platelets by extracellular CyPA.

Mechanistically, Ca<sup>2+</sup> signalling is a central pathway to mediate platelet activation. When human platelets were pretreated with CyPA and subsequently with ADP, we observed a robust increase in intracellular Ca<sup>2+</sup> compared to PBS control. When platelets were pretreated simultaneously with FPS-ZM1, a small-molecule inhibitor for RAGE, CyPA failed to induce relevant intracellular Ca<sup>2+</sup> release (Figure 6B) upon ADP stimulation, indicating that RAGE plays an important role in CyPA-mediated activation of platelets.

These results were confirmed when investigating thrombus formation *in vitro*. CyPA-stimulated human whole blood was perfused over collagen-coated coverslips inducing robust thrombus formation, which was diminished when RAGE, CD147, or both were blocked by adding respective antibodies (Figure 6C).

Bridging the gap between leucocytes and platelets, we furthermore examined whether RAGE is involved in the formation of CyPA-induced platelet–leucocyte co-aggregates. Here, we observed that CyPA increased co-aggregate formation and that blocking of RAGE, CD147, or both with respective antibodies but not an IgG control resulted in a blunted response of human cells (Figure 6D).

As receptor expression on platelets could differ in RAGE-deficient mice, we analysed the surface expression of several activation markers and adhesion molecules on platelets from *Ager*<sup>-/-</sup> and wild-type mice. Platelets from *Ager*<sup>-/-</sup> mice showed no difference in CD147 expression compared to wild-type mice (Figure 7A). Platelets from *Ager*<sup>-/-</sup> mice furthermore showed an unaltered CD62P activation upon stimulation with thrombin compared to wild-type mice. However, a reduced platelet activation regarding surface expression of CD62P and activated GPIIb/IIIa in *Ager*<sup>-/-</sup> mice after treatment with CyPA was observed (Figure 7B and C). Other surface markers, including CD29, CD41a, CD42b, and CD49b, were similar in platelets of *Ager*<sup>-/-</sup> mice compared to wild-type mice and not affected by stimulation with CyPA in both mice (Figure 7D).

RAGE deficiency consequently had a prominent effect on CyPA-induced thrombus formation. Treatment of whole blood of *Ager*<sup>-/-</sup> mice with CyPA resulted in a strongly reduced thrombus formation *in vitro* compared to wild-type mice (Figure 7E).

With these results, we demonstrate that the RAGE receptor plays a central role in facilitating CyPA-induced platelet activation and thrombus formation. In conjunction with the presented data from leucocytes, we characterize a stringent and congruent biological concept for the RAGE receptor in CyPA-induced thrombo-inflammation in leucocytes and platelets.

## 4. Discussion

The present study unravels RAGE as a novel receptor for extracellular CyPA in vascular thrombo-inflammation and shows that (i) CyPA binds to RAGE on the cell surface, (ii) CyPA induces downstream signalling through RAGE via MyD88 activation, NF- $\kappa$ B translocation, and intracellular Ca<sup>2+</sup> release in leucocytes and platelets, and (iii) RAGE expression is induced by extracellular CyPA and drives CyPA-mediated inflammation *in vivo* (also see [Graphical Abstract](#)).

The role of extracellular CyPA has been thoroughly investigated, especially in the context of inflammatory diseases and thrombosis,<sup>4,17–19,57–60</sup>

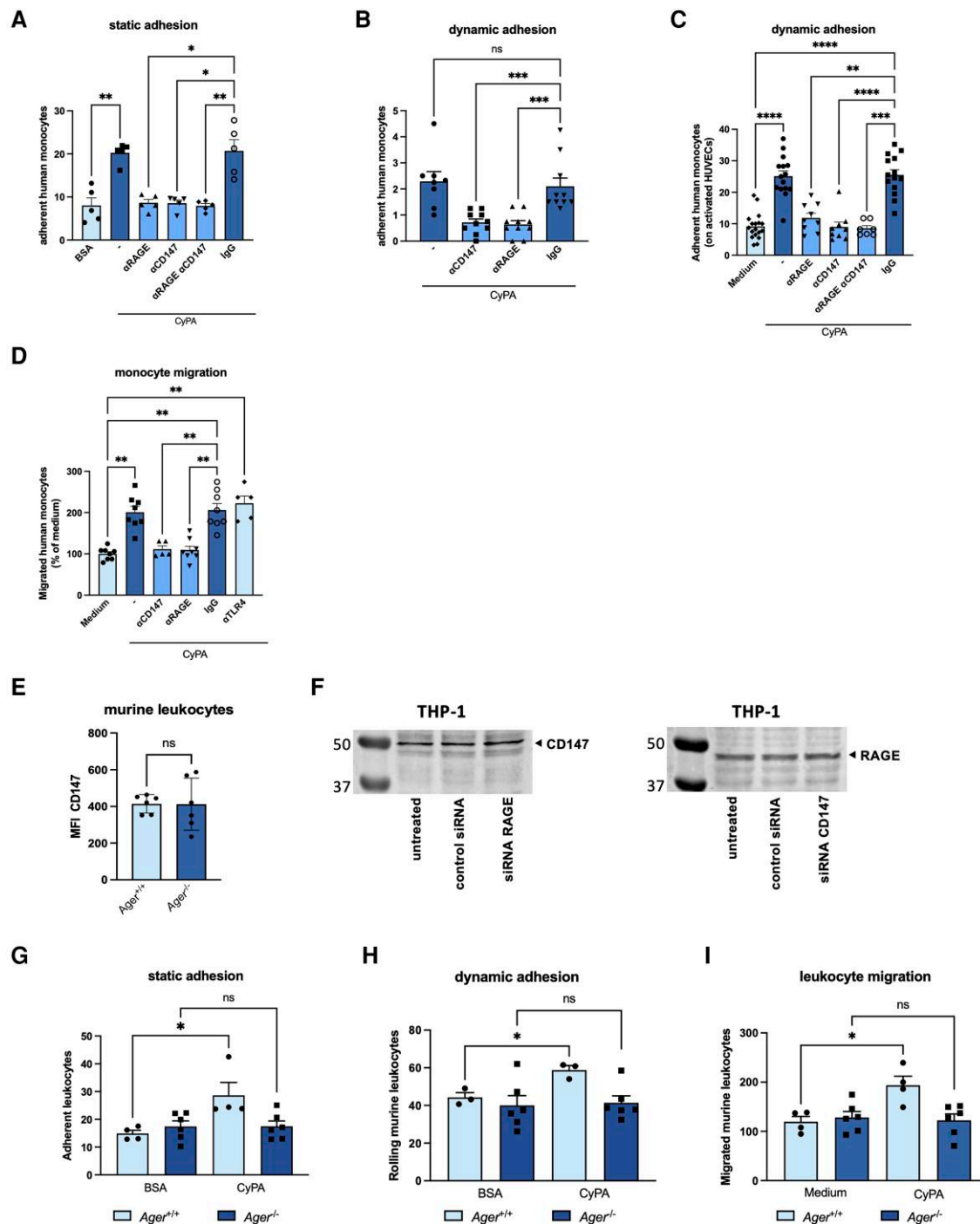


**Figure 4** CyPA-induced leucocyte adhesion and migration are dependent on RAGE. Human monocytes were allowed to adhere to recombinant CyPA or BSA in a static adhesion model. Addition of antibodies against RAGE, CD147, or both (20 µg/mL) abrogated migration towards CyPA (200 nM) (A,  $n = 5$  biological replicates, Kruskal–Wallis test). Under flow conditions, human monocytes showed a diminished adhesion on CyPA-coated surfaces (B,  $n \geq 8$  biological replicates, Kruskal–Wallis test) and activated HUVECs (C,  $n \geq 7$  biological replicates, ANOVA) when RAGE, CD147, or both were blocked with respective antibodies (20 µg/mL). Migration of human monocytes towards CyPA (200 nM) was likewise inhibited when RAGE or CD147 was blocked with antibodies (20 µg/mL), while anti-TLR4 (20 µg/mL) allowed normal migration towards CyPA (D,  $n \geq 5$  biological replicates, Kruskal–Wallis test). *Ager*<sup>-/-</sup> mice showed similar levels of CD147 using flow cytometry (E,  $n = 6$  biological replicates, *t*-test). Similarly, knockdown of RAGE or CD147 using siRNA (1 µM) did not alter the expression of the respective other receptor in THP-1 cells compared to untreated cells or cells transfected with control siRNA (F, representative western blot of three biological replicates is shown). Murine leukocytes from wild-type mice showed robust adhesion on CyPA-coated surfaces in static (G,  $n \geq 4$  biological replicates, Mann–Whitney test, *t*-test) and dynamic conditions (H,  $n \geq 3$  biological replicates, *t*-test) as well as leucocyte migration (I,  $n \geq 4$  biological replicates, *t*-test), while *Ager*<sup>-/-</sup> leucocytes failed to adhere and migrate towards CyPA (200 nM). \* indicates  $P < 0.05$ , \*\* indicates  $P < 0.01$ , \*\*\* indicates  $P < 0.001$ , \*\*\*\* indicates  $P < 0.0001$ , and ns indicates  $P > 0.05$ .

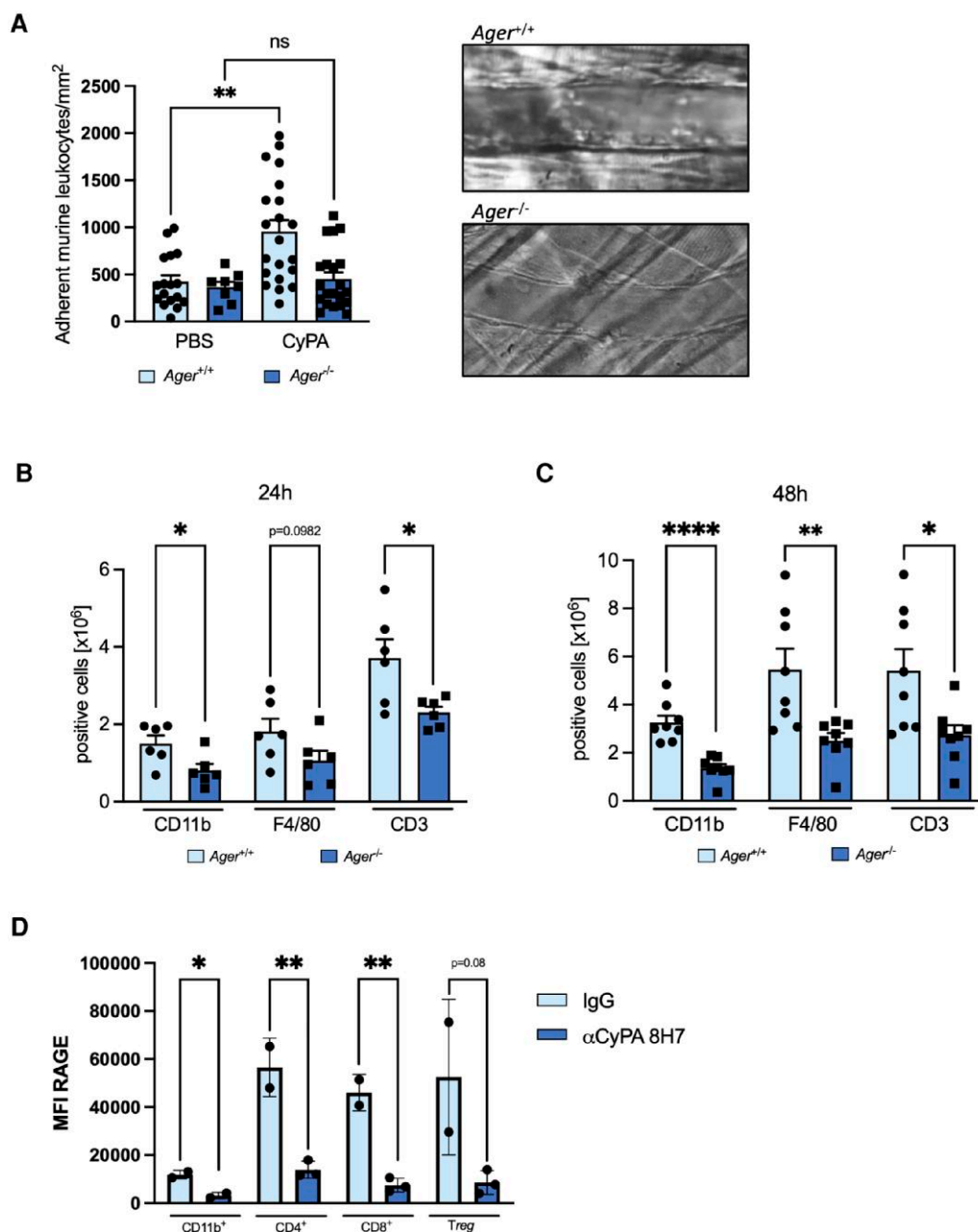


**Figure 5** RAGE is necessary for CyPA-induced leucocyte adhesion and migration and is in turn regulated by extracellular CyPA *in vivo*. In wild-type mice, intravital microscopy revealed a robust adhesion of leucocytes to the postcapillary venules of the cremaster muscle 2 h after intrascrotal injection of CyPA. RAGE-deficient mice showed no increased adhesion after stimulation with CyPA (A,  $n \geq 4$  biological replicates, Mann–Whitney test). Panels on the right show representative images of postcapillary venules from RAGE-deficient and wild-type mice. To evaluate whether RAGE is involved in CyPA-induced leucocyte migration *in vivo*, a CyPA-induced peritonitis model was used where mice were intraperitoneally injected with 10  $\mu$ g CyPA. After 24 (B,  $n = 6$  biological replicates, t-test) or 48 h (C,  $n = 8$  biological replicates, t-test, Mann–Whitney test), mice were sacrificed, and a peritoneal lavage was performed. Isolated cells were stained for CD11b, F4/80, and CD3 and were analysed using flow cytometry. When the basal level of circulating CyPA in mice was reduced by administration of the anti-CyPA antibody 8H7 (5  $\mu$ g/kg) for 24 h, we observed a downregulation of RAGE on CD11b, CD4, CD8, and Treg leucocytes compared to IgG control (5  $\mu$ g/kg), demonstrating a positive feedback loop between CyPA and RAGE (D,  $n \geq 2$  biological replicates, t-test). \* shows  $P < 0.05$ , \*\* shows  $P < 0.01$ , \*\*\*\* shows  $P < 0.0001$ , and ns indicates  $P > 0.05$ .

with the primarily reported receptor for extracellular CyPA being the matrix metalloproteinase inducer CD147.<sup>61</sup> Hibino *et al.*<sup>21</sup> furthermore suggested an interaction of CD147 with S100A9, a calcium-binding protein known to bind RAGE. Due to the importance of RAGE for cardiovascular diseases and diabetes, we were very intrigued to explore

whether RAGE can also bind CyPA, as a crosslink of these previously unrelated receptors has deep implications on our understanding of cardiovascular pathophysiology.

Our immunofluorescence studies indicated a similar expression of RAGE on the cell surface of leucocytes, compared to the known CyPA

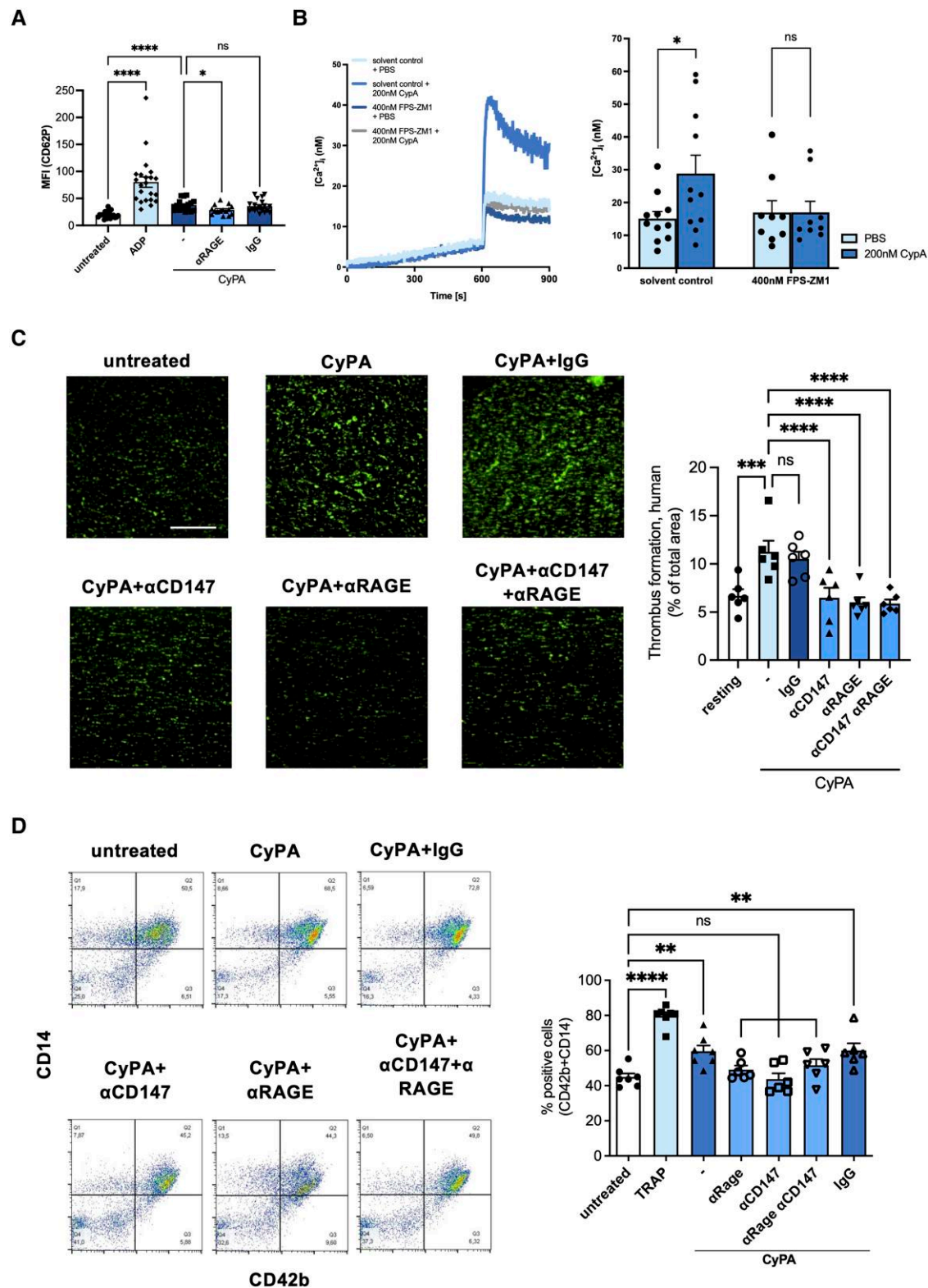


**Figure 6** Inhibition of RAGE blocks CyPA-induced platelet activation via reduced intracellular Ca<sup>2+</sup>. Activation of platelets demonstrated by CD62p surface expression upon CyPA stimulation (200 nM) was diminished in the presence of anti-RAGE antibody (20 μg/mL; A, n ≥ 15 biological replicates, Kruskal–Wallis test, ADP 20 μM). CyPA-induced (200 nM) increase in cytosolic Ca<sup>2+</sup> was abolished by addition of the RAGE inhibitor FPS-ZM1 (400 nM; B, n ≥ 9 biological replicates, t-test; Mann–Whitney test). Antibodies against CD147, RAGE, or both receptors (all 20 μg/mL) reduced CyPA-induced (200 nM) *in vitro* thrombus formation when human whole blood was perfused over fibrinogen-coated surfaces (C, n = 6 biological replicates, ANOVA). Co-aggregation of human platelets and CD14-positive cells after stimulation with CyPA (200 nM) and TRAP (25 μM) was assessed using flow cytometry. When antibodies against RAGE, CD147, or both (all 20 μg/mL) were added, no relevant CyPA-induced co-aggregation was observed (D, n ≥ 6 biological replicates, ANOVA). \* indicates P < 0.05, \*\* indicates P < 0.01, \*\*\* indicates P < 0.001, \*\*\*\* indicates P < 0.0001, and ns indicates P > 0.05.

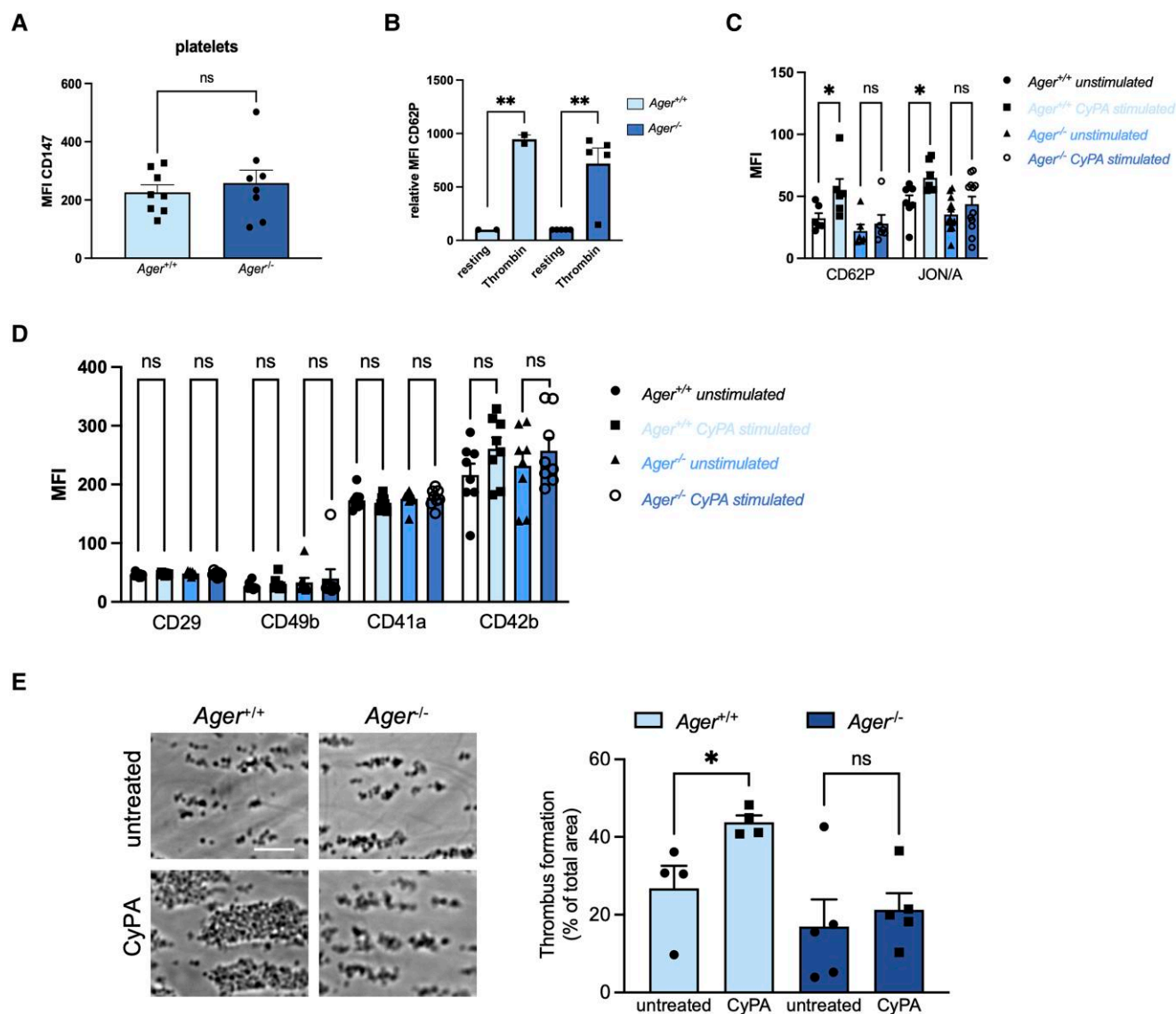


**Figure 7** RAGE-deficient platelets show reduced activation upon CyPA stimulation. Platelets from  $Ager^{-/-}$  mice showed no altered CD147 expression compared to platelets from wild-type mice (A,  $n = 8$  biological replicates, *t*-test). Wild-type and RAGE-deficient platelets showed normal activation after stimulation with thrombin (1 U/mL; B,  $n \geq 2$  biological replicates, *t*-test, Mann–Whitney test). CyPA-induced activation (200 nM) of CD62P and JON/A was diminished in RAGE-deficient platelets, whereas platelets from wild-type mice showed significant activation (C,  $n \geq 6$  biological replicates, *t*-test, Mann–Whitney test). Surface expression of CD29, CD49b, CD41a, and CD42b was not altered after stimulation with CyPA (200 nM) in either genotype (D,  $n \geq 6$ , *t*-test, Mann–Whitney test). CyPA-induced (200 nM) *in vitro* thrombus formation was furthermore dramatically decreased in blood from  $Ager^{-/-}$ , while wild-type mice showed robust thrombus formation (E,  $n \geq 4$ , *t*-test). \* indicates  $P < 0.05$ , \*\* indicates  $P < 0.01$ , and ns indicates  $P > 0.05$ .

receptor CD147. Using proximity ligation, two-colour *d*STORM, and Lattice SIM super-resolution microscopy, we were able to reveal a spatial association of CyPA with RAGE at the range of 50–100 nm. While these experiments established a very close proximity on the cell surface, we were interested to see whether CyPA and RAGE directly interact with each other.

Using RAGE-CHO cells, we were able to measure the change in adhesion force and adhesion work introduced by RAGE overexpression on the cell surface to immobilized CyPA. The force needed to lift a CyPA-coated cantilever from the cell surface of RAGE-CHO cells was found to be significantly greater than from parental CHO-cells, which demonstrates direct interaction and a significant strength of the interaction on the cell surface. The interaction was furthermore confirmed using co-immunoprecipitation and binding ELISAs.

Circulating RAGE isoforms can act as decoy receptors inhibiting ligand–RAGE interactions on the cell surface.<sup>53,54</sup> When CyPA was preincubated with recombinant RAGE, we observed a markedly reduced chemotaxis compared to CyPA alone, which mimics the findings of circulating sRAGE by providing a sink for ligands before interacting with RAGE on the cell surface and therefore omitting downstream signalling.

When investigating the role of RAGE for the chemotactic activity of extracellular CyPA, we observed that inhibition of RAGE abrogates the migration of leucocytes as well as adhesion of leucocytes under static and under flow conditions, similarly to inhibition of CD147. The results were confirmed by leucocytes from  $Ager^{-/-}$  mice showing no relevant migration towards CyPA while retaining their migratory abilities towards other chemoattractants, therefore exhibiting no general migratory defect.

Furthermore, we confirmed that leucocytes from *Ager*<sup>-/-</sup> mice showed similar CD147 expression levels compared to wild-type mice to rule out reduced CD147 expression resulting in the reported effects. Similarly, knockdown of CD147 or RAGE also did not result in a reciprocal regulation of the respective other receptor in THP-1 cells. Other investigators have performed extensive RNA sequencing analyses in *Ager*<sup>-/-</sup> vs. wild-type mice and congruently did not observe CD147 (*Bsg*) to be differentially regulated in macrophages *in vivo*.<sup>62</sup>

The CyPA–RAGE interaction proved to play a significant role *in vivo* as well, which was demonstrated using a CyPA-induced peritonitis model. Here, *Ager*<sup>-/-</sup> mice showed a lower leucocyte recruitment upon CyPA injection compared to wild-type mice. The results highlight the strong dependence of CyPA-induced leucocyte migration on RAGE signalling, which previously was described only to be dependent on CD147 interaction.

As RAGE is known to facilitate leucocyte recruitment to the vessel wall,<sup>63</sup> we investigated the role of RAGE for CyPA-mediated adhesion of leucocytes. The interaction with CyPA under flow conditions was reduced when cells were RAGE deficient or RAGE was blocked, indicating that RAGE is a necessary player for CyPA-induced leucocyte adhesion. Perfusing human monocytes in combination with antibodies against CD147 and/or RAGE over immobilized CyPA or activated HUVECs, as well as murine *Ager*<sup>-/-</sup> leucocytes over immobilized CyPA, resulted in reduced cellular adhesion. In the next step, we probed the *in vivo* adhesion of leucocytes to postcapillary venules of the cremaster muscle in mice to mimic leucocyte recruitment driven by CyPA. After intrascrotal injection of CyPA, wild-type mice showed an elevated adhesion of leucocytes to the endothelium. Adhesion upon CyPA stimulation was markedly reduced in *Ager*<sup>-/-</sup> mice, indicating that RAGE is indeed necessary for CyPA-induced leucocyte recruitment to the vessel wall *in vivo*.

*In vivo*, inflammation is driven by many different mediators and signalling molecules that orchestrate the response to a proinflammatory stimulus in parallel. Within this proinflammatory cocktail, key downstream targets are often activated by more than one receptor or signalling pathway. In the case of CD147 and RAGE, this proved even more complicated, as both receptors are able to recognize many different proinflammatory ligands that are commonly released in proinflammatory settings *in vivo* (including HMGB1, S100 proteins, CyPB, integrins, and GPVI), rendering the dissection of the mechanisms involved very challenging. We found no feasible way to selectively induce only a release of CyPA *in vivo*, while making sure that no other ligand of RAGE or CD147 was released or induced leading to a proinflammatory response that could mimic the effect of extracellular CyPA. We therefore exploited the fact that numerous studies have shown positive feedback loops that regulate the expression of RAGE (reviewed in Ott *et al.*<sup>55</sup> and Jang *et al.*<sup>64</sup>) depending on ligand abundance. To investigate this effect, we selectively neutralized the basal endogenous extracellular CyPA *in vivo* by i.p. administration of the CyPA-binding antibody 8H7. We expected that a decrease of available basal endogenous extracellular CyPA for 24 h would result in a decrease of RAGE on the cell surface of leucocytes. Indeed, we observed that leucocytes showed a dramatic decrease in RAGE surface expression upon inhibition of endogenous extracellular CyPA *in vivo*. We observed this effect not only on one leucocyte subset but on CD11b<sup>+</sup>, CD4<sup>+</sup>, CD8<sup>+</sup>, and regulatory T cells. These data provide novel evidence that extracellular CyPA is an important regulatory factor for RAGE on leucocytes *in vivo*. However, it is not feasible to thoroughly exclude that other ligands of RAGE are involved in the manner of a superligand induction state but together with the binding analyses and the *in vitro* studies, the evidence we provide supports that RAGE may bind CyPA. This is especially interesting as many diseases have been associated with increased RAGE expression in parallel with increased circulating CyPA levels, including myocardial infarction and thrombosis, as well as chronic inflammation and diabetes.<sup>20,65</sup> The understanding of this feed-forward mechanism where CyPA increases RAGE expression on leucocytes presents an important link in understanding the pathophysiology and dynamics of acute inflammatory processes as well as chronification of inflammation. Furthermore, the CyPA–RAGE interaction establishes an important link regarding thrombo-inflammation.

Regarding thrombosis, CyPA has previously been found to be critically involved in platelet activation, intracellular calcium homeostasis, and thrombosis via CD147.<sup>18,58</sup> RAGE has similarly been identified to be involved in platelet activation *in vivo*, as well as venous and arterial thrombosis by S100, HMGB1, and AGEs.<sup>31–33</sup>

Following stimulation with CyPA platelets showed an increased  $\alpha$ -granule secretion (surface expression of CD62P) and integrin  $\alpha_{IIb}\beta_3$  activation. In line with the results detailed above, inhibition of the CyPA–RAGE interaction reduced the surface expression of CD62P and activated integrin  $\alpha_{IIb}\beta_3$  and resulted in a decreased ability to form thrombi in murine as well as human whole blood, indicating that pro-thrombotic effects of CyPA are not exclusively mediated by CD147 but also rely on CyPA–RAGE interaction. Consequently, CyPA-induced co-aggregation of platelets with leucocytes was diminished by the inhibition of RAGE as well.

Platelets react with a marked increase in cytosolic Ca<sup>2+</sup> abundance when activated with extracellular CyPA. As intracellular Ca<sup>2+</sup> release in platelets is a central and tightly regulated step in platelet activation, we were interested to see whether Ca<sup>2+</sup> abundance in platelets was altered by inhibition of RAGE upon stimulation with extracellular CyPA. As expected, extracellular CyPA induced a robust increase in intracellular Ca<sup>2+</sup> levels, which was blunted by RAGE inhibition. The CyPA–RAGE interaction may therefore play a critical role in CyPA-induced platelet activation. Especially in cardiovascular disorders, liberation of CyPA has been well documented,<sup>20</sup> and RAGE has likewise been identified to be upregulated and augment pathophysiological processes in these conditions. Increased levels of circulating CyPA in combination with abundantly expressed RAGE could therefore play a clinically important role in augmenting inflammation and platelet activation as driving forces of cardiovascular events. Hence, it is tempting to speculate that targeted interference with the CyPA–RAGE interaction could be a promising therapeutic strategy for chronic inflammation and thrombo-inflammation.

As CyPA also induces several downstream signalling pathways in leucocytes, we investigated whether RAGE is necessary for their initiation.<sup>17,55,66–69</sup> We demonstrate that the RAGE-binding adaptor protein MyD88 is crucially involved in CyPA-mediated migration, while CD147 shares no known interaction with MyD88.<sup>70,71</sup> It is important to note that *MyD88*<sup>-/-</sup> leucocytes maintained normal chemotaxis towards SDF1, which rules out a general migration defect of these cells while interfering with the RAGE–MyD88 axis abrogated chemotaxis towards CyPA. We were intrigued to observe that blocking of RAGE by FPS-ZM1 or RAP, as well as CD147 by antibody or SP8356, resulted in a diminished MyD88 activation. Further downstream, we observed similar results where NF- $\kappa$ B activation was blunted by inhibition of RAGE or CD147. The CyPA–RAGE interaction therefore seems to have a prominent effect on the proinflammatory MyD88–NF- $\kappa$ B axis, which leads to increased production of cytokines and chemokines, adhesion molecules, and inflammatory regulation.<sup>72</sup> Through additional RAGE signalling, CyPA therefore has a wider range of influence on multiple aspects of innate and adaptive immune functions than only through CD147.

The RAGE receptor consists of three domains V, C1, and C2 that form the extracellular region and a short transmembrane as well as a cytoplasmic signal domain. The V domain is an immunoglobulin-like domain found to be the binding site for AGEs, S100, and HMGB1. The V domain forms a constructive unit with the C1 domain, while the C2 domain is independently attached to the VC1 domain. FPS-ZM1 (*N*-benzyl-*N*-cyclohexyl-4-chlorobenzamide) inhibits the interaction between the V domain and several ligands. Similarly, the S100-derived RAP competes for the RAGE site required for binding these ligands.<sup>73</sup> As both FPS-ZM1 and RAP were found to effectively decrease CyPA-induced cellular effects, it is very likely that CyPA relies on the V domain to activate RAGE downstream signalling, which was confirmed by *in silico* protein complex modelling.

Our data clearly show that both receptors interact with extracellular CyPA and that both receptors are required for CyPA-dependent cell signalling. Signalling through activation of RAGE and CD147 has previously been found to be of unexpected complexity. For CD147, a metabolic activation complex has been uncovered that consists, in addition to CD147, of amino acid transporters 4F2hc, LAT1, and ASCT2 (SLC1A5), a

Na<sup>+</sup>/K<sup>+</sup>-ATPase, and the cell adhesion mediators EpCAM and integrin β1, which are termed a 'metabolon', as reviewed in Fairweather et al.<sup>34</sup> Similarly, RAGE has been shown to be transactivated by the angiotensin II receptor AT<sub>1</sub> and plays a complex role beyond mere ligand binding in the directional crosstalk enabling downstream signal transduction.<sup>35,74</sup>

A limitation to be considered is that while we confirmed that RAGE deficiency did not influence CD147 expression on murine leucocytes and platelets, we have not investigated the expression of RAGE on CD147-deficient cells. However, siRNA knockdown of RAGE or CD147 did not reciprocally change the expression of the other receptor in THP-1 cells. As the RAGE pathway has a complex signalling network with respect to its ligand repertoire, we also cannot rule out that other ligands or pathways are involved in the signal transduction of CyPA.

In the light of these mechanisms and the data we present, we postulate that successful CyPA signalling depends on binding to RAGE and CD147 to induce downstream signal transduction in a 'signalosome'<sup>75</sup> fashion, explaining why dual inhibition of both receptors resulted in no additional reduction in several experiments shown, compared to inhibition of a single receptor. The presented data lead to the conclusion that both receptors are necessary at the same time or in close succession in order to facilitate CyPA-mediated effects. We anticipate that future studies will uncover the exact mechanisms of the CyPA–RAGE–CD147 interaction, of which all three play prominent roles in highly relevant pathologies of today.

## Supplementary material

Supplementary material is available at *Cardiovascular Research* online.

## Author contributions

Substantial contributions to the conception or design of the work or the acquisition, analysis, or interpretation of data for the work: P.S., S.N.I.v.U.-S., V.D., V.H., A.R., E.B., M.N., A.-K.R., M.S., P.P.N., C.N., M.Sp., C.K., M.M., M.Sa., P.M., K.B., A.S., A.F.M., R.H., K.B., M.L., R.F., A.P., K.K., T.E.S., B.N., O.B., A.E.M., A.Z., M.G., and D.H. Drafting the work or revising it critically for important intellectual content: P.S., S.N.I.v.U.-S., V.D., V.H., A.R., E.B., M.N., A.-K.R., M.S., P.P.N., C.N., M.Sp., C.K., M.M., M.Sa., P.M., K.B., A.S., A.F.M., R.H., K.B., M.L., R.F., A.P., K.K., T.E.S., B.N., O.B., A.E.M., A.Z., M.G., and D.H. Final approval of the version to be published: P.S., S.N.I.v.U.-S., V.D., V.H., A.R., E.B., M.N., A.-K.R., M.S., P.P.N., C.N., M.Sp., C.K., M.M., M.Sa., P.M., K.B., A.S., A.F.M., R.H., K.B., M.L., R.F., A.P., K.K., T.E.S., B.N., O.B., A.E.M., A.Z., M.G., and D.H. Agreement to be accountable for all aspects of the work in ensuring that questions related to the accuracy or integrity of any part of the work are appropriately investigated and resolved: P.S., S.N.I.v.U.-S., V.D., V.H., A.R., E.B., M.N., A.-K.R., M.S., P.P.N., C.N., M.Sp., C.K., M.M., M.Sa., P.M., K.B., A.S., A.F.M., R.H., K.B., M.L., R.F., A.P., K.K., T.E.S., B.N., O.B., A.E.M., A.Z., M.G., and D.H.

## Acknowledgements

We thank PD Dr. Erwin Bohn (Institute of Microbiology and Infection Medicine, Eberhard Karls University Tübingen, Tübingen, Germany), for providing MyD88 knockout mice, and Dr. Miroslav Malešević (Martin-Luther-University Halle-Wittenberg, Institute of Biochemistry and Biotechnology, Enzymology Department, Halle, Germany) and Prof. Dr. Gunter Fischer (Max Planck Institute for Biophysical Chemistry, Göttingen, Germany), for providing MM284. We thank Klaudia Posavec, Sarah Gekeler, Daniela Eißler, and Carole Maleck for providing outstanding technical support. The graphical abstract was created using biorender.com.

**Conflict of interest:** D.H. received compensation for travel expenses and participation fees from Abbott and speaker fees from Pfizer.

## Funding

This work was supported by grants from the German Research Foundation [Deutsche Forschungsgemeinschaft, DFG #374031971-TRR 240 CRU-240, BO3786/3-1, BO3786/7-1, SFB 1118, #335549539-GRK2381, INST 37/1133-1FUGG, TRR332 project C02 (M.Sp.)], the Deutsche Stiftung für Herzforschung (DH), and the German Center for Diabetes Research. The sponsors played no role in study design, collection, analysis, and interpretation of data, in the writing of the report, and in the decision to submit the article for publication.

## Data availability

The data underlying this article are available in the article and in its online [Supplementary material](#).

## References

1. Lv M, Miao J, Zhao P, Luo X, Han Q, Wu Z, Zhang K, Zhu P. CD147-mediated chemotaxis of CD4(+)CD161(+) T cells may contribute to local inflammation in rheumatoid arthritis. *Clin Rheumatol* 2018;**37**:59–66.
2. Seizer P, Ochmann C, Schönberger T, Zach S, Rose M, Borst O, Klingel K, Kandolf R, MacDonald HR, Nowak RA, Engelhardt S, Lang F, Gawaz M, May AE. Disrupting the EMMPRIN (CD147)-cyclophilin A interaction reduces infarct size and preserves systolic function after myocardial ischemia and reperfusion. *Arterioscler Thromb Vasc Biol* 2011;**31**:1377–1386.
3. Seizer P, Schönberger T, Schott M, Lang MR, Langer HF, Bigalke B, Kramer BF, Borst O, Daub K, Heidenreich O, Schmidt R, Lindemann S, Herouy Y, Gawaz M, May AE. EMMPRIN and its ligand cyclophilin A regulate MT1-MMP, MMP-9 and M-CSF during foam cell formation. *Atherosclerosis* 2010;**209**:51–57.
4. Heinzmann D, Bangert A, Müller AM, von Ungern-Sternberg SN, Emschermann F, Schönberger T, Chatterjee M, Mack AF, Klingel K, Kandolf R, Malešević M, Borst O, Gawaz M, Langer HF, Katus H, Fischer G, May AE, Kaya Z, Seizer P. The novel extracellular cyclophilin A (CyPA)—inhibitor MM284 reduces myocardial inflammation and remodeling in a mouse model of troponin I-induced myocarditis. *PLoS One* 2015;**10**:e0124606.
5. Rasaiyaah J, Tan CP, Fletcher AJ, Price AJ, Blondeau C, Hilditch L, Jacques DA, Selwood DL, James LC, Noursadeghi M, Towers GJ. HIV-1 evades innate immune recognition through specific cofactor recruitment. *Nature* 2013;**503**:402–405.
6. Saleh T, Jankowski W, Sriram G, Rossi P, Shah S, Lee KB, Cruz LA, Rodriguez AJ, Birge RB, Kalodimos CG. Cyclophilin A promotes cell migration via the Abl-Crk signaling pathway. *Nat Chem Biol* 2016;**12**:117–123.
7. Villmow M, Baumann M, Malešević M, Sachs R, Hause G, Fändrich M, Balbach J, Schiene-Fischer C. Inhibition of Abeta(1-40) fibril formation by cyclophilins. *Biochem J* 2016;**473**:1355–1368.
8. Stemmy EJ, Benton AS, Lerner J, Alcalá S, Constant SL, Freishtat RJ. Extracellular cyclophilin levels associate with parameters of asthma in phenotypic clusters. *J Asthma* 2011;**48**:986–993.
9. Xue C, Sowden M, Berk BC. Extracellular cyclophilin A, especially acetylated, causes pulmonary hypertension by stimulating endothelial apoptosis, redox stress, and inflammation. *Arterioscler Thromb Vasc Biol* 2017;**37**:1138–1146.
10. Nigro P, Satoh K, O'Dell MR, Soe NN, Cui Z, Mohan A, Abe J, Alexis JD, Sparks JD, Berk BC. Cyclophilin A is an inflammatory mediator that promotes atherosclerosis in apolipoprotein E-deficient mice. *J Exp Med* 2011;**208**:53–66.
11. Satoh K, Nigro P, Berk BC. Oxidative stress and vascular smooth muscle cell growth: a mechanistic linkage by cyclophilin A. *Antioxid Redox Signal* 2010;**12**:675–682.
12. Kim SH, Lessner SM, Sakurai Y, Galis ZS. Cyclophilin A as a novel biphasic mediator of endothelial activation and dysfunction. *Am J Pathol* 2004;**164**:1567–1574.
13. Christofferson DE, Yuan J. Cyclophilin A release as a biomarker of necrotic cell death. *Cell Death Differ* 2010;**17**:1942–1943.
14. Manke MC, Geue S, Coman C, Peng B, Kollotzek F, Münzer P, Walker B, Huber SM, Rath D, Sickmann A, Stegner D, Duerschmied D, Lang F, Nieswandt B, Gawaz M, Ahrends R, Borst O. ANXA7 regulates platelet lipid metabolism and Ca<sup>2+</sup> release in arterial thrombosis. *Circ Res* 2021;**129**:494–507.
15. Schutte JP, Manke MC, Hemmen K, Munzer P, Schorg BF, Ramos GC, Pogoda M, Dicenta V, Hoffmann SHL, Pinnecker J, Kollotzek F, Zdanyte M, Mueller KAL, Singh Y, Mack AF, Pichler B, Lang F, Nieswandt B, Gawaz M, Heinze KG, Casadei N, Borst O. Platelet-derived microRNAs regulate cardiac remodeling after myocardial ischemia. *Circ Res* 2023;**132**:e96–e113.
16. Hoffmann H, Schiene-Fischer C. Functional aspects of extracellular cyclophilins. *Biol Chem* 2014;**395**:721–735.
17. Seizer P, Ungern-Sternberg SN, Schönberger T, Borst O, Munzer P, Schmidt EM, Mack AF, Heinzmann D, Chatterjee M, Langer H, Malešević M, Lang F, Gawaz M, Fischer G, May AE. Extracellular cyclophilin A activates platelets via EMMPRIN (CD147) and PI3K/Akt signaling, which promotes platelet adhesion and thrombus formation in vitro and in vivo. *Arterioscler Thromb Vasc Biol* 2015;**35**:655–663.
18. von Ungern-Sternberg SNI, Vogel S, Walker-Allgaier B, Geue S, Maurer A, Wild AM, Münzer P, Chatterjee M, Heinzmann D, Kremmer E, Borst O, Loughran P, Zerneck A, Neal MD,



- Billiar TR, Gawaz M, Seizer P. Extracellular cyclophilin A augments platelet-dependent thrombosis and thromboinflammation. *Thromb Haemost* 2017;**117**:2063–2078.
19. Gawaz M, Langer H, May AE. Platelets in inflammation and atherogenesis. *J Clin Invest* 2005;**115**:3378–3384.
  20. Seizer P, Gawaz M, May AE. Cyclophilin A and EMMPRIN (CD147) in cardiovascular diseases. *Cardiovasc Res* 2014;**102**:17–23.
  21. Hibino T, Sakaguchi M, Miyamoto S, Yamamoto M, Motoyama A, Hosoi J, Shimokata T, Ito T, Tsuboi R, Huh NH. S100a9 is a novel ligand of EMMPRIN that promotes melanoma metastasis. *Cancer Res* 2013;**73**:172–183.
  22. Alexaki VI, May AE, Fujii C, V Ungern-Sternberg Saskia N, Mund C, Gawaz M, Chavakis T, Seizer P. S100a9 induces monocyte/macrophage migration via EMMPRIN. *Thromb Haemost* 2017;**117**:636–639.
  23. Srikrishna G, Freeze HH. Endogenous damage-associated molecular pattern molecules at the crossroads of inflammation and cancer. *Neoplasia* 2009;**11**:615–628.
  24. Leclerc E, Vetter SW. The role of S100 proteins and their receptor RAGE in pancreatic cancer. *Biochim Biophys Acta* 2015;**1852**:2706–2711.
  25. Neeper M, Schmidt AM, Brett J, Yan SD, Wang F, Pan YC, Elliston K, Stern D, Shaw A. Cloning and expression of a cell surface receptor for advanced glycosylation end products of proteins. *J Biol Chem* 1992;**267**:14998–15004.
  26. Wu X, Mi Y, Yang H, Hu A, Zhang Q, Shang C. The activation of HMGB1 as a progression factor on inflammation response in normal human bronchial epithelial cells through RAGE/JNK/NF-kappaB pathway. *Mol Cell Biochem* 2013;**380**:249–257.
  27. Yan SD, Chen X, Fu J, Chen M, Zhu H, Roher A, Slattery T, Zhao L, Nagashima M, Morser J, Migheli A, Nawroth P, Stern D, Schmidt AM. RAGE and amyloid-beta peptide neurotoxicity in Alzheimer's disease. *Nature* 1996;**382**:685–691.
  28. Frommhold D, Kamphues A, Hepper I, Pruenster M, Lukić IK, Socher I, Zablotzka V, Buschmann K, Lange-Sperandio B, Schymeinsky J, Ryschich E, Poeschl J, Kupatt C, Nawroth PP, Moser M, Walzog B, Bierhaus A, Sperandio M. RAGE and ICAM-1 cooperate in mediating leukocyte recruitment during acute inflammation in vivo. *Blood* 2010;**116**:841–849.
  29. Oczypok EA, Perkins TN, Oury TD. All the "RAGE" in lung disease: the receptor for advanced glycation endproducts (RAGE) is a major mediator of pulmonary inflammatory responses. *Paediatr Respir Rev* 2017;**23**:40–49.
  30. Recabarren-Leiva D, Burgos CF, Hernandez B, Garcia-Garcia FJ, Castro RI, Guzman L, Fuentes E, Palomo I, Alarcon M. Effects of the age/rage axis in the platelet activation. *Int J Biol Macromol* 2021;**166**:1149–1161.
  31. Ortilion J, Hezard N, Belmokhtar K, Kaweck C, Terryn C, Fritz G, Kauskot A, Schmidt AM, Rieu P, Nguyen P, Maurice P, Toure F. Receptor for advanced glycation end products is involved in platelet hyperactivation and arterial thrombosis during chronic kidney disease. *Thromb Haemost* 2020;**120**:1300–1312.
  32. Ahrens I, Chen YC, Topcic D, Bode M, Haenel D, Hagemeyer CE, Seeba H, Duerschmied D, Bassler N, Jandeleit-Dahm KA, Sweet MJ, Agrotis A, Bobik A, Peter K. HMGB1 binds to activated platelets via the receptor for advanced glycation end products and is present in platelet rich human coronary artery thrombi. *Thromb Haemost* 2015;**114**:994–1003.
  33. Stark K, Philippi V, Stockhausen S, Busse J, Antonelli A, Miller M, Schubert I, Hoseinpour P, Chandraratne S, von Bruhl ML, Gaertner F, Lorenz M, Agresti A, Coletti R, Antoine DJ, Heermann R, Jung K, Reese S, Laitinen I, Schwaiger M, Walch A, Sperandio M, Nawroth PP, Reinhardt C, Jackel S, Bianchi ME, Massberg S. Disulfide HMGB1 derived from platelets coordinates venous thrombosis in mice. *Blood* 2016;**128**:2435–2449.
  34. Fairweather SJ, Shah N, Bröer S. Heteromeric solute carriers: function, structure, pathology and pharmacology. *Adv Exp Med Biol* 2021;**21**:13–127.
  35. Pickering RJ, Tikellis C, Rosado CJ, Tsorotes D, Dimitropoulos A, Smith M, Huet O, Seeber RM, Abhayawardana R, Johnstone EK, Golledge J, Wang Y, Jandeleit-Dahm KA, Cooper ME, Pflieger KD, Thomas MC. Transactivation of RAGE mediates angiotensin-induced inflammation and atherogenesis. *J Clin Invest* 2019;**129**:406–421.
  36. Schmidt AM, Yan SD, Yan SF, Stern DM. The multiligand receptor RAGE as a progression factor amplifying immune and inflammatory responses. *J Clin Invest* 2001;**108**:949–955.
  37. Perkins TN, Oczypok EA, Dutz RE, Donnell ML, Myerburg MM, Oury TD. The receptor for advanced glycation end products is a critical mediator of type 2 cytokine signaling in the lungs. *J Allergy Clin Immunol* 2019;**144**:796–808.e12.
  38. Martens HA, Nienhuis HL, Gross S, van der Steege G, Brouwer E, Berden JH, de Sevaux RG, Derksen RH, Voskuyl AE, Berger SP, Navis GJ, Nolte IM, Kallenberg CG, Bijl M. Receptor for advanced glycation end products (RAGE) polymorphisms are associated with systemic lupus erythematosus and disease severity in lupus nephritis. *Lupus* 2012;**21**:959–968.
  39. Stritt S, Birkholz I, Beck S, Sorrentino S, Sappal KT, Vlaud J, Heck J, Gaits-Iacovoni F, Schulze H, Du X, Hartwig JH, Braun A, Bender M, Medalia O, Nieswandt B. Profilin 1-mediated cytoskeletal rearrangements regulate integrin function in mouse platelets. *Blood Adv* 2018;**2**:1040–1045.
  40. Volz J, Kusch C, Beck S, Popp M, Vogtle T, Meub M, Scheller I, Heil HS, Preu J, Schuhmann MK, Hemmen K, Premster T, Sickmann A, Heinze KG, Stegner D, Stoll G, Braun A, Sauer M, Nieswandt B. BIN2 orchestrates platelet calcium signaling in thrombosis and thrombo-inflammation. *J Clin Invest* 2020;**130**:6064–6079.
  41. Babu M, Favretto F, de Opakua AI, Rankovic M, Becker S, Zwickstetter M. Proline/arginine dipeptide repeat polymers derail protein folding in amyotrophic lateral sclerosis. *Nat Commun* 2021;**12**:3396.
  42. Yatime L, Betzer C, Jensen RK, Mortensen S, Jensen PH, Andersen GR. The structure of the RAGEs:100A6 complex reveals a unique mode of homodimerization for S100 proteins. *Structure* 2016;**24**:2043–2052.
  43. Friesner RA, Banks JL, Murphy RB, Halgren TA, Klicic JJ, Mainz DT, Repasky MP, Knoll EH, Shelley M, Perry JK, Shaw DE, Francis P, Shenkin PS. Glide: a new approach for rapid, accurate docking and scoring. 1. Method and assessment of docking accuracy. *J Med Chem* 2004;**47**:1739–1749.
  44. Eble JA. Titration ELISA as a method to determine the dissociation constant of receptor ligand and interaction. *J Vis Exp* 2018;**132**:57334.
  45. Seizer P, Borst O, Langer HF, Bultmann A, Munch G, Herouy Y, Stellos K, Kramer B, Bigalke B, Buchele B, Bachem MG, Vestweber D, Simmet T, Gawaz M, May AE. EMMPRIN (CD147) is a novel receptor for platelet GPVI and mediates platelet rolling via GPVI-EMMPRIN interaction. *Thromb Haemost* 2009;**101**:682–686.
  46. Luo Y, Hara T, Ishido Y, Yoshihara A, Oda K, Makino M, Ishii N, Hiroi N, Suzuki K. Rapid preparation of high-purity nuclear proteins from a small number of cultured cells for use in electrophoretic mobility shift assays. *BMC Immunol* 2014;**15**:586.
  47. Pries AR. A versatile video image analysis system for microcirculatory research. *Int J Microcirc Clin Exp* 1988;**7**:327–345.
  48. Long DS, Smith ML, Pries AR, Ley K, Damiano ER. Microviscosimetry reveals reduced blood viscosity and altered shear rate and shear stress profiles in microvessels after hemodilution. *Proc Natl Acad Sci USA* 2004;**101**:10060–10065.
  49. Borst O, Munzer P, Gatidis S, Schmidt EM, Schonberger T, Schmid E, Towhid ST, Stellos K, Seizer P, May AE, Lang F, Gawaz M. The inflammatory chemokine CXC motif ligand 16 triggers platelet activation and adhesion via CXC motif receptor 6-dependent phosphatidylinositol 3-kinase/Akt signaling. *Circ Res* 2012;**111**:1297–1307.
  50. Deane R, Singh I, Sagare AP, Bell RD, Ross NT, LaRue B, Love R, Perry S, Paquette N, Deane RJ, Thiagarajan M, Zaccaro T, Fritz G, Friedman AE, Miller BL, Zlokovic BV. A multimodal RAGE-specific inhibitor reduces amyloid beta-mediated brain disorder in a mouse model of Alzheimer disease. *J Clin Invest* 2012;**122**:1377–1392.
  51. Arumugam T, Ramachandran V, Gomez SB, Schmidt AM, Logsdon CD. S100P-derived RAGE antagonistic peptide reduces tumor growth and metastasis. *Clin Cancer Res* 2012;**18**:4356–4364.
  52. Hecht FM, Rheinlaender J, Schierbaum N, Goldmann WH, Fabry B, Schaffer TE. Imaging viscoelastic properties of live cells by AFM: power-law rheology on the nanoscale. *Soft Matter* 2015;**11**:4584–4591.
  53. Wendt TM, Tanji N, Guo J, Kislinger TR, Qu W, Lu Y, Bucciarelli LG, Rong LL, Moser B, Markowitz GS, Stein G, Bierhaus A, Liliensiek B, Arnold B, Nawroth PP, Stern DM, D'Agati VD, Schmidt AM. RAGE drives the development of glomerulosclerosis and implicates podocyte activation in the pathogenesis of diabetic nephropathy. *Am J Pathol* 2003;**162**:1123–1137.
  54. Sakaguchi T, Yan SF, Yan SD, Belov D, Rong LL, Sousa M, Andrassy M, Marso SP, Duda S, Arnold B, Liliensiek B, Nawroth PP, Stern DM, Schmidt AM, Naka Y. Central role of RAGE-dependent neointimal expansion in arterial restenosis. *J Clin Invest* 2003;**111**:959–972.
  55. Ott C, Jacobs K, Hauke E, Navarrete Santos A, Grune T, Simm A. Role of advanced glycation end products in cellular signaling. *Redox Biol* 2014;**2**:411–429.
  56. Nishioku T, Dohgu S, Koga M, Machida T, Watanabe T, Miura T, Tsumagari K, Terasawa M, Yamauchi A, Kataoka Y. Cyclophilin A secreted from fibroblast-like synoviocytes is involved in the induction of CD147 expression in macrophages of mice with collagen-induced arthritis. *J Inflamm (Lond)* 2012;**9**:44.
  57. Seizer P, Fuchs C, Ungern-Sternberg SN, Heinzmann D, Langer H, Gawaz M, May AE, Geisler T. Platelet-bound cyclophilin A in patients with stable coronary artery disease and acute myocardial infarction. *Platelets* 2016;**27**:155–158.
  58. Elvers M, Herrmann A, Seizer P, Munzer P, Beck S, Schonberger T, Borst O, Martin-Romero FJ, Lang F, May AE, Gawaz M. Intracellular cyclophilin A is an important Ca(2+) regulator in platelets and critically involved in arterial thrombus formation. *Blood* 2012;**120**:1317–1326.
  59. Billich A, Winkler G, Aschauer H, Rot A, Peichl P. Presence of cyclophilin A in synovial fluids of patients with rheumatoid arthritis. *J Exp Med* 1997;**185**:975–980.
  60. Pasetto L, Pozzi S, Castelnovo M, Basso M, Estevez AG, Fumagalli S, De Simoni MG, Castellaneta V, Bigini P, Restelli E, Chiesa R, Trojsi F, Monsurro MR, Callea L, Malesevic M, Fischer G, Freschi M, Tortarolo M, Bendotti C, Bonetto V. Targeting extracellular cyclophilin A reduces neuroinflammation and extends survival in a mouse model of amyotrophic lateral sclerosis. *J Neurosci* 2017;**37**:1413–1427.
  61. Yurchenko V, Zylbarth G, O'Connor M, Dai WW, Franchin G, Hao T, Guo H, Hung HC, Toole B, Galloway P, Sherry B, Bukrinsky M. Active site residues of cyclophilin A are crucial for its signaling activity via CD147. *J Biol Chem* 2002;**277**:22959–22965.
  62. Senatus L, Lopez-Diez R, Egana-Gorrono L, Liu J, Hu J, Daffu G, Li Q, Rahman K, Vengrenyuk Y, Barrett TJ, Dewan MZ, Guo L, Fuller D, Finn AV, Virmani R, Li H, Friedman RA, Fisher EA, Ramasamy R, Schmidt AM. RAGE impairs murine diabetic atherosclerosis regression and implicates IRF7 in macrophage inflammation and cholesterol metabolism. *JCI Insight* 2020;**5**:e137289.
  63. Ziegler T, Horstkotte M, Lange P, Ng J, Bongiovanni D, Hinkel R, Laugwitz KL, Sperandio M, Horstkotte J, Kupatt C. Endothelial RAGE exacerbates acute postischemic cardiac inflammation. *Thromb Haemost* 2016;**116**:300–308.
  64. Jang EJ, Kim H, Baek SE, Jeon EY, Kim JW, Kim JY, Kim CD. HMGB1 increases RAGE expression in vascular smooth muscle cells via ERK and p-38 MAPK-dependent pathways. *Korean J Physiol Pharmacol* 2022;**26**:389–396.
  65. Ramasamy R, Schmidt AM. Receptor for advanced glycation end products (RAGE) and implications for the pathophysiology of heart failure. *Curr Heart Fail Rep* 2012;**9**:107–116.

66. Kamynina A, Esteras N, Koroev DO, Angelova PR, Volpina OM, Abramov AY. Activation of RAGE leads to the release of glutamate from astrocytes and stimulates calcium signal in neurons. *J Cell Physiol* 2021;**236**:6496–6506.
67. Trachtenberg A, Pushkarsky T, Heine S, Constant S, Brichacek B, Bukrinsky M. The level of CD147 expression correlates with cyclophilin-induced signalling and chemotaxis. *BMC Res Notes* 2011;**4**:396.
68. Schmidt R, Bultmann A, Fischel S, Gillitzer A, Cullen P, Walch A, Jost P, Ungerer M, Tolley ND, Lindemann S, Gawaz M, Schomig A, May AE. Extracellular matrix metalloproteinase inducer (CD147) is a novel receptor on platelets, activates platelets, and augments nuclear factor kappaB-dependent inflammation in monocytes. *Circ Res* 2008;**102**:302–309.
69. Yan SD, Schmidt AM, Anderson GM, Zhang J, Brett J, Zou YS, Pinsky D, Stern D. Enhanced cellular oxidant stress by the interaction of advanced glycation end products with their receptors/binding proteins. *J Biol Chem* 1994;**269**:9889–9897.
70. Sakaguchi M, Murata H, Yamamoto K, Ono T, Sakaguchi Y, Motoyama A, Hibino T, Kataoka K, Huh NH. TIRAP, an adaptor protein for TLR2/4, transduces a signal from RAGE phosphorylated upon ligand binding. *PLoS One* 2011;**6**:e23132.
71. Vogel S, Bodenstern R, Chen Q, Feil S, Feil R, Rheinlaender J, Schaffer TE, Bohn E, Frick JS, Borst O, Munzer P, Walker B, Markel J, Csanyi G, Pagano PJ, Loughran P, Jessup ME, Watkins SC, Bullock GC, Sperry JL, Zuckerbraun BS, Billiar TR, Lotze MT, Gawaz M, Neal MD. Platelet-derived HMGB1 is a critical mediator of thrombosis. *J Clin Invest* 2015;**125**:4638–4654.
72. Liu T, Zhang L, Joo D, Sun SC. NF-kappaB signaling in inflammation. *Signal Transduct Target Ther* 2017;**2**:17023.
73. Kim HJ, Jeong MS, Jang SB. Molecular characteristics of RAGE and advances in small-molecule inhibitors. *Int J Mol Sci* 2021;**22**:6904.
74. Yokoyama S, Kawai T, Yamamoto K, Yibin H, Yamamoto H, Kakino A, Takeshita H, Nozato Y, Fujimoto T, Hongyo K, Takahashi T, Nakagami F, Akasaka H, Takami Y, Takeya Y, Sugimoto K, Sawamura T, Rakugi H. RAGE ligands stimulate angiotensin II type I receptor (AT1) via RAGE/AT1 complex on the cell membrane. *Sci Rep* 2021;**11**:5759.
75. Kandy SK, Janmey PA, Radhakrishnan R. Membrane signalosome: where biophysics meets systems biology. *Curr Opin Syst Biol* 2021;**25**:34–41.

## Translational perspective

Leucocyte recruitment and platelet activation are fundamental steps in clinical conditions ranging from host defence to myocardial infarction. In this manuscript, we identify CyPA as a ubiquitously expressed ligand for RAGE on leucocytes and platelets facilitating platelet activation as well as leucocyte recruitment *in vitro* and *in vivo*. We furthermore identified a feed-forward mechanism between basal CyPA levels and RAGE expression on different leucocyte subsets *in vivo*. The CyPA–RAGE interaction thus represents a novel mechanism facilitating thrombo-inflammation and connecting two important effector molecules.